

## ELECTRONIC SUPPORTING INFORMATION

### *Three-state molecular potentiometer based on a non-symmetrically positioned in-backbone linker*

Lucía Palomino-Ruiz,<sup>‡a,b</sup> Pablo Reiné,<sup>‡a</sup> Irene R. Márquez,<sup>c</sup> Luis Álvarez de Cienfuegos,<sup>a</sup> Nicolás Agraït,<sup>b,d,e</sup> Juan M. Cuerva,<sup>a</sup> Araceli G. Campaña,<sup>a</sup> Edmund Leary,<sup>b</sup> Delia Miguel,<sup>\*f</sup> Alba Millán,<sup>\*a</sup> Linda A. Zotti,<sup>\*e,g</sup> M. Teresa González<sup>\*b</sup>

---

<sup>a.</sup> *Departamento de Química Orgánica, Facultad de Ciencias, Unidad de Excelencia de Química Aplicada a Biomedicina y Medioambiente (UEQ), Universidad de Granada, 18071 Granada, Spain.*

<sup>b.</sup> *Fundación IMDEA Nanociencia, 28049 Madrid, Spain.*

<sup>c.</sup> *Centro de Instrumentación Científica, Universidad de Granada, 18071 Granada, Spain.*

<sup>d.</sup> *Departamento de Física de la Materia Condensada, Universidad Autónoma de Madrid, 28049 Madrid, Spain.*

<sup>e.</sup> *Condensed Matter Physics Center (IFIMAC), Universidad Autónoma de Madrid, 28049 Madrid, Spain.*

<sup>f.</sup> *Departamento de Fisicoquímica, Facultad de Farmacia, Unidad de Excelencia de Química Aplicada a Biomedicina y Medioambiente (UEQ), Universidad de Granada, 18071 Granada, Spain.*

<sup>g.</sup> *Departamento de Física Teórica de la Materia Condensada, Universidad Autónoma de Madrid, 28049 Madrid, Spain.*

---

#### TABLE OF CONTENTS

<b>1. Synthesis of compounds.....</b>	<b>S2</b>
- <i>General details.....</i>	S2
- <i>Synthesis and characterization of building blocks.....</i>	S3
- <i>Synthesis and characterization of main compounds.....</i>	S9
<b>2. <sup>1</sup>H and <sup>13</sup>C spectra of new compounds.....</b>	<b>S14</b>
<b>3. Break-junction experiments.....</b>	<b>S25</b>
- <i>Data analysis.....</i>	S25
- <i>Additional clustering analysis.....</i>	S26
- <i>Conductance of OPE4-OMe.....</i>	S27
- <i>Conductance for OPE3/S-pym.....</i>	S29
- <i>Conductance for OPE2/S-pym.....</i>	S30
<b>4. Additional theoretical calculations.....</b>	<b>S31</b>

---

## 1. SYNTHESIS OF COMPOUNDS

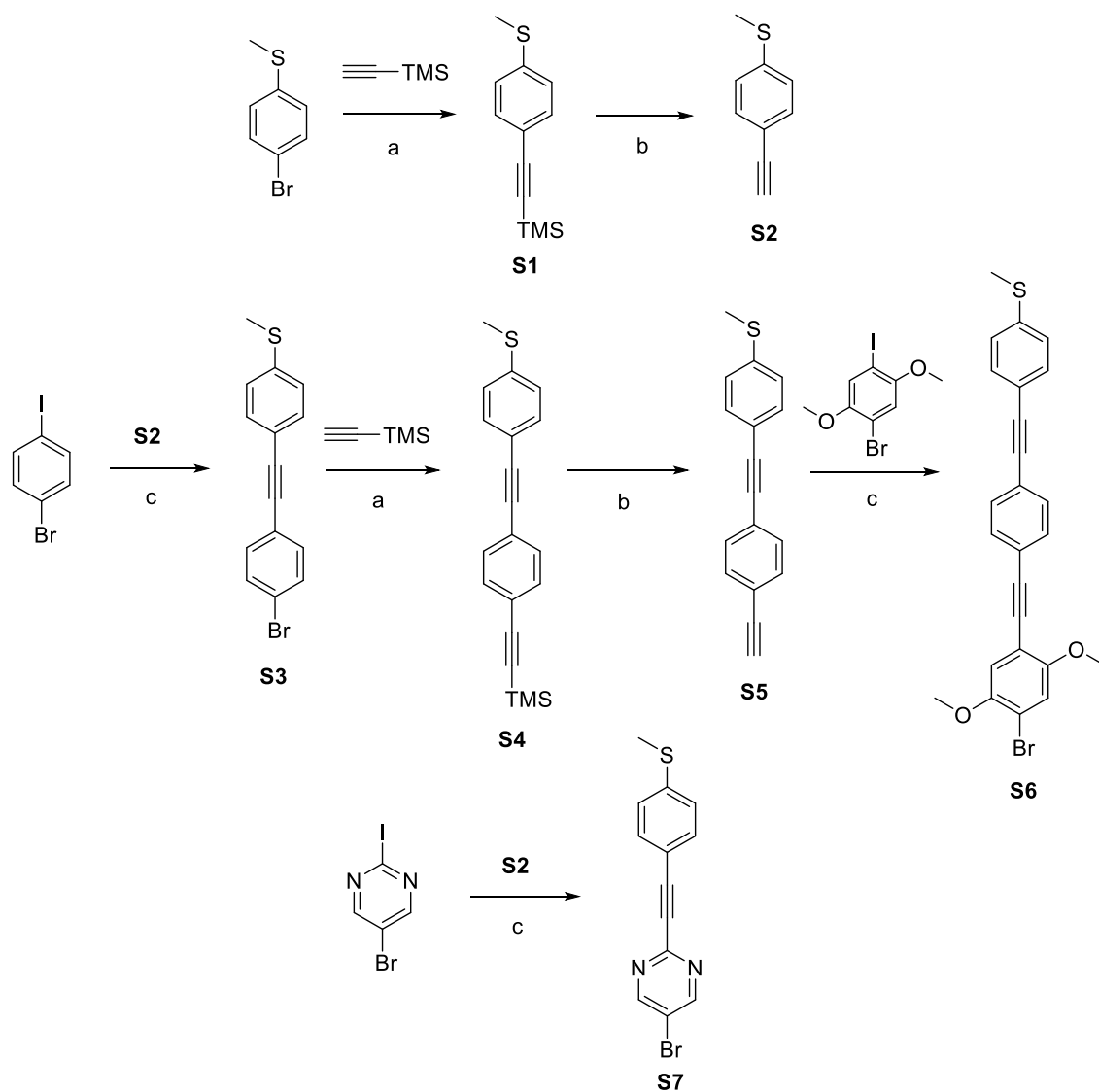
### *General Details*

The following palladium catalysts, trans-dichlorobis(triphenylphosphine) palladium(II) ( $\text{Pd}(\text{PPh}_3)_2\text{Cl}_2$ ) and trans-dichlorobis(acetonitrile)palladium(II) ( $\text{Pd}(\text{CH}_3\text{CN})_2\text{Cl}_2$ ), were prepared from palladium(II) chloride ( $\text{PdCl}_2$ ) according to previously described procedures.<sup>1</sup> All reagents and solvents ( $\text{CH}_2\text{Cl}_2$ , EtOAc, hexane, THF,  $\text{iPr}_2\text{NH}$ ,  $\text{Et}_3\text{N}$ ) were purchased from standard chemical suppliers and used without further purification. Dry THF was freshly distilled over Na/benzophenone. Thin-layer chromatography analysis was performed on aluminium-backed plates coated with silica gel 60 (230-240 mesh) with F254 indicator. The spots were visualized with UV light (254 nm and 360 nm) and/or stained with phosphomolybdic acid (10% ethanol solution) and subsequent heating. Chromatography purifications were performed with silica gel 60 (40-63  $\mu\text{m}$ ).  $^1\text{H}$  and  $^{13}\text{C}$  NMR spectra were recorded on Varian 400 or 500 MHz spectrometers, at a constant temperature of 298 K. Chemical shifts are reported in ppm using residual solvent peak as reference ( $\text{CDCl}_3$ :  $\delta = 7.26$  ppm,  $\text{CD}_2\text{Cl}_2$ :  $\delta = 5.32$  ppm). Data are reported as follows: chemical shift, multiplicity (s: singlet, d: doublet, t: triplet, dd: doublet of doublets), coupling constant ( $J$  in Hz) and integration. Coupling constants refer to apparent multiplicities and not true coupling constants.  $^{13}\text{C}$  NMR spectra were recorded at 101 or 126 MHz using broadband proton decoupling and chemical shifts are reported in ppm using residual solvent peaks as reference ( $\text{CDCl}_3$ :  $\delta = 77.16$  ppm,  $\text{CD}_2\text{Cl}_2$ :  $\delta = 54.00$  ppm). Carbon multiplicities were accomplished by DEPT techniques. High-resolution mass spectra (HRMS) were recorded using EI on a Micromass GCT Agilent Technologies 6890N (Waters), by APCI mass spectra carried out on a Bruker MAXIS II mass spectrometer or by ESI mass spectrometry carried out on a Waters Xevo G2-XS QToF mass spectrometer.

---

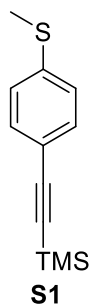
<sup>1</sup> N. Miyaura and A. Suzuki, *J. Chem. Soc., Chem. Commun.*, 1979, 866.

### Synthesis and characterization of building blocks



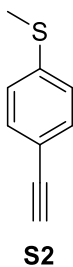
**Scheme S1.** Synthesis of building blocks. a)  $\text{Pd}(\text{CH}_3\text{CN})_2\text{Cl}_2$ ,  $t\text{Bu}_3\text{P}\cdot\text{HBF}_4$ ,  $\text{CuI}$ ,  $i\text{Pr}_2\text{NH}/\text{THF}$ , rt. b)  $\text{Bu}_4\text{NF}$ ,  $\text{THF}$ , rt. c)  $\text{Pd}(\text{PPh}_3)_2\text{Cl}_2$ ,  $\text{CuI}$ ,  $\text{Et}_3\text{N}/\text{THF}$ , rt.

### Compound S1.



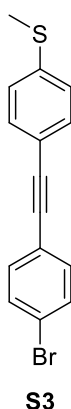
Trimethylsilyl acetylene (3.86 g, 40 mmol) dissolved in 10 mL of THF was added dropwise to a carefully degassed solution of  $\text{Pd}(\text{CH}_3\text{CN})_2\text{Cl}_2$  (240 mg, 1 mmol), CuI (180 mg, 1 mmol),  $t\text{Bu}_3\text{P}\cdot\text{HBF}_4$  (460 mg, 2 mmol) and 4-bromothioanisole (4 g, 20 mmol) in 30 mL of  $i\text{Pr}_2\text{NH}$ . Afterwards, the reaction was stirred at room temperature under argon atmosphere during 24 h. The mixture was then diluted with EtOAc and washed with saturated aq  $\text{NH}_4\text{Cl}$  solution. The organic layer was dried over anhydrous  $\text{Na}_2\text{SO}_4$  and the solvent removed under reduced pressure. The residue was purified by flash chromatography ( $\text{SiO}_2$ , Hexane) to give **S1** (4.16 g, 96%) as a yellow oil.  $\delta^1\text{H NMR}$  (400 MHz;  $\text{CDCl}_3$ ) 7.37 (d,  $J = 8.6$  Hz, 2H), 7.15 (d,  $J = 8.6$  Hz, 2H), 2.48 (s, 3H), 0.24 (s, 9H).  $\delta^{13}\text{C NMR}$  (101 MHz;  $\text{CDCl}_3$ ) 139.7 (C), 132.4 (CH), 125.8 (CH), 119.6 (C), 105.0 (C), 94.3 (C), 15.5 ( $\text{CH}_3$ ), 0.1 ( $\text{CH}_3$ ). HRMS (EI):  $m/z$   $[\text{M}]^+$  calcd for  $\text{C}_{12}\text{H}_{16}\text{SiS}$ : 220.0742; found: 220.0737.

### Compound S2.



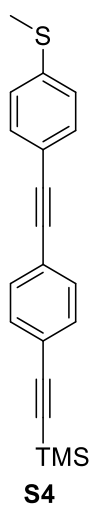
To a solution of **S1** (4.16 g, 18.9 mmol) in THF (20 ml) with 4-5 drops of water,  $\text{Bu}_4\text{NF}$  (8.9 g, 28.3 mmol) was added, and the mixture was stirred at room temperature until complete consumption of the starting material (TLC, 1 h). The solution was then diluted with EtOAc and washed with brine. The organic layer was dried over anhydrous  $\text{Na}_2\text{SO}_4$  and the solvent removed under reduced pressure. The residue was purified by flash chromatography ( $\text{SiO}_2$ , Hexane) to give **S2** (2.27 g, 82%) as a yellow oil.  $\delta^1\text{H NMR}$  (400 MHz;  $\text{CDCl}_3$ ) 7.40 (d,  $J = 8.1$  Hz, 2H), 7.18 (d,  $J = 8.1$  Hz, 2H), 3.07 (s, 1H), 2.48 (s, 3H).  $\delta^{13}\text{C NMR}$  (101 MHz;  $\text{CDCl}_3$ ) 140.2(C), 132.5 (CH), 125.9 (CH), 118.5 (C), 83.6 (C), 77.3 (CH), 15.5( $\text{CH}_3$ ). HRMS (EI):  $m/z$   $[\text{M}]^+$  calcd for  $\text{C}_9\text{H}_8\text{S}$ : 148.0347; found: 148.0346.

### Compound S3.



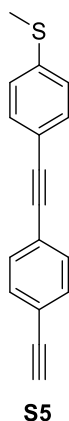
A solution of **S2** (618 mg, 4.2 mmol) dissolved in 2 mL of THF was added dropwise during 1 h to a carefully degassed solution of Pd(PPh<sub>3</sub>)<sub>2</sub>Cl<sub>2</sub> (123 mg, 0.17 mmol), CuI (33 mg, 0.17 mmol) and 1-bromo-4-iodobenzene (1 g, 3.5 mmol) in 8 mL of Et<sub>3</sub>N. Afterwards, the reaction was stirred at room temperature under argon atmosphere during 2 h. The mixture was then diluted with EtOAc and washed with saturated aq NH<sub>4</sub>Cl solution. The organic layer was dried over anhydrous Na<sub>2</sub>SO<sub>4</sub> and the solvent removed under reduced pressure. The residue was purified by flash chromatography (SiO<sub>2</sub>, Hexane) to give **S3** (1.14 g, 99%) as a yellow solid.  $\delta$  <sup>1</sup>H NMR (400 MHz; CDCl<sub>3</sub>) 7.48 (d, *J* = 8.6 Hz, 2H), 7.43 (d, *J* = 8.6 Hz, 2H), 7.37 (d, *J* = 8.5 Hz, 2H), 7.21 (d, *J* = 8.5 Hz, 2H), 2.50 (s, 3H).  $\delta$  <sup>13</sup>C NMR (101 MHz; CDCl<sub>3</sub>) 139.5 (C), 132.8 (CH), 131.7 (CH), 131.4 (CH), 125.7 (CH), 122.2 (C), 122.1 (C), 119.0 (C), 90.2 (C), 88.2 (C), 15.2 (CH<sub>3</sub>). HRMS (EI): *m/z* [M]<sup>+</sup> calcd for C<sub>15</sub>H<sub>11</sub>SBr: 301.9765; found: 301.9772.

### Compound S4.



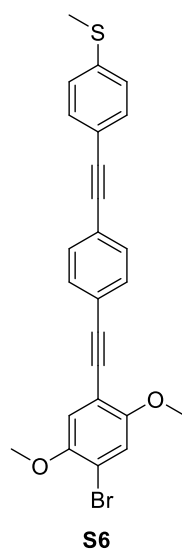
Trimethylsilyl acetylene (721 mg, 7.36 mmol) was added dropwise to a carefully degassed solution of Pd(CH<sub>3</sub>CN)<sub>2</sub>Cl<sub>2</sub> (48 mg, 0.18 mmol), CuI (35 mg, 0.18 mmol), tBu<sub>3</sub>P·HBF<sub>4</sub> (107 mg, 0.37 mmol) and **S3** (1.11 g, 3.68 mmol) in 10 mL of *i*Pr<sub>2</sub>NH and 15 mL of THF. Afterwards, the reaction was stirred at room temperature under argon atmosphere during 24 h. The mixture was then diluted with EtOAc and washed with saturated aq NH<sub>4</sub>Cl solution. The organic layer was dried over anhydrous Na<sub>2</sub>SO<sub>4</sub> and the solvent removed under reduced pressure. The residue was purified by flash chromatography (SiO<sub>2</sub>, Hexane) to give **S4** (1.44 g, 99%) as a yellow solid.  $\delta$  <sup>1</sup>H NMR (400 MHz; CDCl<sub>3</sub>) 7.44 (s, 4H), 7.42 (d, *J* = 8.5 Hz, 2H), 7.21 (d, *J* = 8.5 Hz, 2H), 2.50 (s, 3H), 0.26 (s, 9H).  $\delta$  <sup>13</sup>C NMR (101 MHz; CDCl<sub>3</sub>) 139.8 (C), 132.04 (CH), 132.01 (CH), 131.4 (CH), 126.0 (CH), 123.5 (C), 122.9 (C), 119.4 (C), 104.8 (C), 96.4 (C), 91.3 (C), 89.3 (C), 15.5 (CH<sub>3</sub>), 0.1 (CH<sub>3</sub>). HRMS (EI): *m/z* [M]<sup>+</sup> calcd for C<sub>20</sub>H<sub>20</sub>SiS: 320.1055; found: 320.1040.

#### Compound S5.



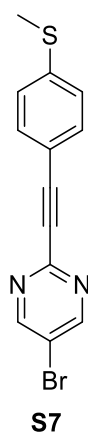
To a solution of **S4** (920 mg, 2.87 mmol) in THF (10 mL) with 4-5 drops of water, Bu<sub>4</sub>NF (1.36 g, 4.3 mmol) was added, and the mixture was stirred at room temperature until complete consumption of the starting material (TLC, 1 h). The solution was then diluted with EtOAc and washed with brine. The organic layer was dried over anhydrous Na<sub>2</sub>SO<sub>4</sub> and the solvent removed under reduced pressure. The residue was purified by flash chromatography (SiO<sub>2</sub>, Hexane) to give **S5** (536 mg, 75%) as a yellow solid.  $\delta$  <sup>1</sup>H NMR (400 MHz; CDCl<sub>3</sub>) 7.46 (s, 4H), 7.43 (d, *J* = 8.6 Hz, 2H), 7.21 (d, *J* = 8.6 Hz, 2H), 3.17 (s, 1H), 2.50 (s, 3H).  $\delta$  <sup>13</sup>C NMR (101 MHz; CDCl<sub>3</sub>) 139.9 (C), 132.2 (CH), 132.0 (CH), 131.5 (CH), 126.0 (CH), 124.0 (C), 121.9 (C), 119.3 (C), 91.4 (C), 89.1 (C), 83.4 (C), 79.0 (CH), 15.5 (CH<sub>3</sub>). HRMS (EI): *m/z* [M]<sup>+</sup> calcd for C<sub>17</sub>H<sub>12</sub>S: 248.0660; found: 248.0666.

## Compound S6.



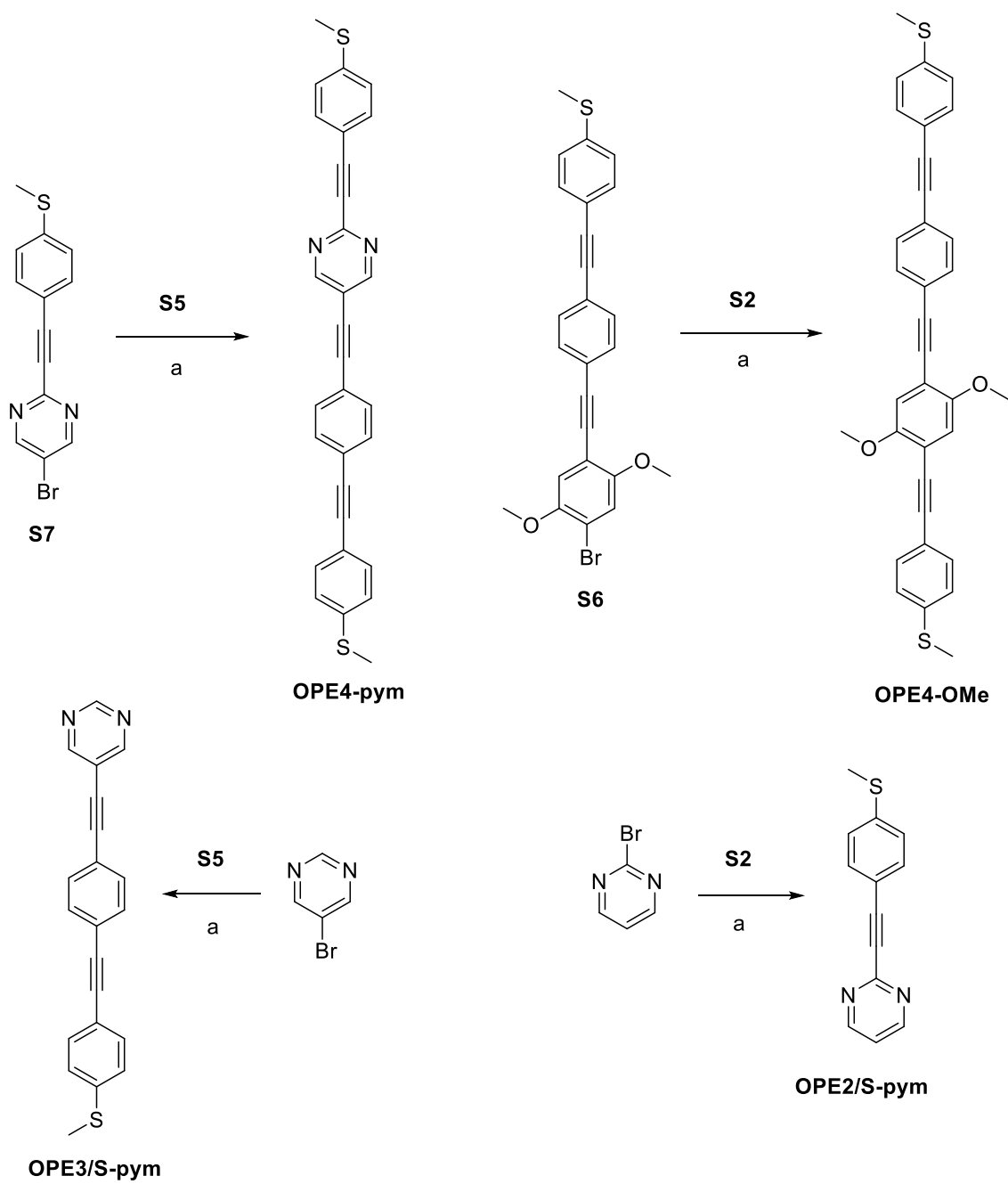
A solution of **S5** (254 mg, 1.02 mmol) in 3 mL of THF was added dropwise to a carefully degassed solution of Pd(PPh<sub>3</sub>)<sub>2</sub>Cl<sub>2</sub> (35 mg, 0.05 mmol), CuI (19 mg, 0.1 mmol) and 1-bromo-4-iodo-2,5-dimethoxybenzene (318 mg, 3.5 mmol) in 4 mL of Et<sub>3</sub>N. Afterwards, the reaction was stirred at room temperature under argon atmosphere overnight. The mixture was then diluted with EtOAc and washed with saturated aq NH<sub>4</sub>Cl solution. The organic layer was dried over anhydrous Na<sub>2</sub>SO<sub>4</sub> and the solvent removed under reduced pressure. The residue was purified by flash chromatography (SiO<sub>2</sub>, EtOAc/Hexane 1:9) to give **S6** (202 mg, 47%) as a yellow solid.  $\delta$  <sup>1</sup>H NMR (500 MHz; CDCl<sub>3</sub>) 7.53 (d, *J* = 8.5 Hz, 2H), 7.49 (d, *J* = 8.5 Hz, 2H), 7.44 (d, *J* = 8.5 Hz, 2H), 7.21 (d, *J* = 8.5 Hz, 2H), 7.12 (s, 1H), 7.03 (s, 1H), 3.88 (s, 6H), 2.50 (s, 3H).  $\delta$  <sup>13</sup>C NMR (126 MHz; CDCl<sub>3</sub>) 154.7 (C), 150.0 (C), 139.8 (C), 132.0 (CH), 131.7 (CH), 131.6 (CH), 126.0 (CH), 123.4 (C), 123.0 (C), 119.4 (C), 116.7 (CH), 116.5 (CH), 113.0 (C), 112.0 (C), 94.1 (C), 91.4 (C), 89.4 (C), 87.1 (C), 57.0 (CH<sub>3</sub>), 56.8 (CH<sub>3</sub>), 15.5 (CH<sub>3</sub>). HRMS (ESI): *m/z* [M+H]<sup>+</sup> calcd. for C<sub>25</sub>H<sub>20</sub>O<sub>2</sub>SBr: 465.0347; found: 465.0330.

## Compound S7.



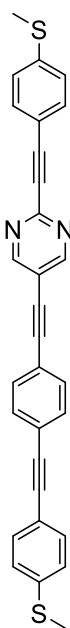
A solution of **S2** (258 mg, 1.75 mmol) in 8 mL of THF was added dropwise to a carefully degassed solution of Pd(PPh<sub>3</sub>)<sub>2</sub>Cl<sub>2</sub> (62 mg, 0.09 mmol), CuI (17 mg, 0.09 mmol) and 5-bromo-2-iodopyrimidine (500 mg, 1.75 mmol) in 5 mL of Et<sub>3</sub>N. Afterwards, the reaction was stirred at room temperature under argon atmosphere overnight. The mixture was then diluted with EtOAc and washed with saturated aq NH<sub>4</sub>Cl solution. The organic layer was dried over anhydrous Na<sub>2</sub>SO<sub>4</sub> and the solvent removed under reduced pressure. The residue was purified by flash chromatography (SiO<sub>2</sub>, EtOAc/Hexane 3:7) to give **S7** (360 mg, 68%) as a yellow solid.  $\delta$  <sup>1</sup>H NMR (400 MHz; CDCl<sub>3</sub>) 8.79 (s, 2H), 7.56 (d, *J* = 8.5 Hz, 2H), 7.22 (d, *J* = 8.5 Hz, 2H), 2.51 (s, 3H).  $\delta$  <sup>13</sup>C NMR (101 MHz; CDCl<sub>3</sub>) 158.2 (CH), 151.3 (C), 142.1 (C), 133.0 (CH), 125.7 (CH), 119.0 (C), 117.1 (C), 89.7 (C), 87.6 (C), 15.2 (CH<sub>3</sub>). HRMS (ESI): *m/z* [M+H]<sup>+</sup> calcd. for C<sub>13</sub>H<sub>10</sub>N<sub>2</sub>SBr: 304.9748; found: 304.9748.

Synthesis and characterization of main compounds



**Scheme S2.** Synthesis of main compounds. a)  $\text{Pd}(\text{CH}_3\text{CN})_2\text{Cl}_2$ ,  $t\text{Bu}_3\text{P}\cdot\text{HBF}_4$ ,  $\text{CuI}$ ,  $i\text{Pr}_2\text{NH}/\text{THF}$ , rt.

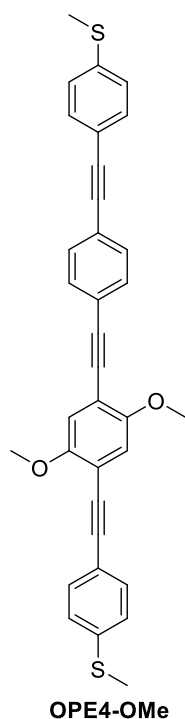
**Compound OPE4-pym.**



**OPE4-pym**

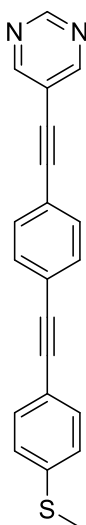
A solution of **S5** (293 mg, 1.18 mmol) dissolved in 5 mL of THF was added dropwise to a carefully degassed solution of Pd(CH<sub>3</sub>CN)<sub>2</sub>Cl<sub>2</sub> (31 mg, 0.12 mmol), CuI (23 mg, 0.12 mmol), *t*Bu<sub>3</sub>P·HBF<sub>4</sub> (70 mg, 0.24 mmol) and **S7** (360 mg, 1.18 mmol) in 4 mL of *i*Pr<sub>2</sub>NH. Afterwards, the reaction was stirred at room temperature under argon atmosphere during 24 h. The mixture was then diluted with CH<sub>2</sub>Cl<sub>2</sub> and washed with saturated aq NH<sub>4</sub>Cl solution. The organic layer was dried over anhydrous Na<sub>2</sub>SO<sub>4</sub> and the solvent removed under reduced pressure. The residue was purified by flash chromatography (SiO<sub>2</sub>, EtOAc/Hexane 2:8) and then CH<sub>2</sub>Cl<sub>2</sub> to give **OPE4-pym** (10 mg, 2%) as a light green solid.  $\delta$  <sup>1</sup>H NMR (500 MHz; CD<sub>2</sub>Cl<sub>2</sub>) 8.84 (s, 2H), 7.56 (d, *J* = 3.2 Hz, 6H), 7.46 (d, *J* = 8.4 Hz, 2H), 7.26 (d, *J* = 8.5 Hz, 2H), 7.24 (d, *J* = 8.4 Hz, 2H), 2.52 (s, 3H), 2.51 (s, 3H).  $\delta$  <sup>13</sup>C NMR (126 MHz; CD<sub>2</sub>Cl<sub>2</sub>) 159.5 (CH), 151.4 (C), 142.8 (C), 140.9 (C), 133.3 (CH), 132.4 (CH), 132.3 (CH), 132.1 (CH), 126.3 (CH), 126.1 (CH), 125.0 (C), 122.1 (C), 119.4 (C), 118.2 (C), 117.6 (C), 97.6 (C), 92.3 (C), 90.1 (C), 89.3 (C), 87.3 (C), 85.1 (C), 15.6 (CH<sub>3</sub>), 15.4 (CH<sub>3</sub>). HRMS (ES): *m/z* [M+H]<sup>+</sup> calcd for C<sub>30</sub>H<sub>21</sub>N<sub>2</sub>S<sub>2</sub>: 473.1146; found: 473.1133.

**Compound OPE4-OMe.**



A solution of **S2** (71 mg, 0.48 mmol) dissolved in 4 mL of THF was added dropwise to a carefully degassed solution of Pd(CH<sub>3</sub>CN)<sub>2</sub>Cl<sub>2</sub> (10 mg, 0.04 mmol), CuI (10 mg, 0.05 mmol), *t*Bu<sub>3</sub>P·HBF<sub>4</sub> (20 mg, 0.07 mmol) and **S6** (202 mg, 0.44 mmol) in 5 mL of *i*Pr<sub>2</sub>NH. Afterwards, the reaction was stirred at room temperature under argon atmosphere during 24 h. The mixture was then diluted with EtOAc and washed with saturated aq NH<sub>4</sub>Cl solution. The organic layer was dried over anhydrous Na<sub>2</sub>SO<sub>4</sub> and the solvent removed under reduced pressure. The residue was purified by flash chromatography (SiO<sub>2</sub>, EtOAc/Hexane 2:98) to give **OPE4-OMe** (18 mg, 8%) as a white solid.  $\delta$  <sup>1</sup>H NMR (500 MHz; CDCl<sub>3</sub>)  $\delta$  7.54 (d, *J* = 8.5 Hz, 2H), 7.51-7.46 (m, 4H), 7.44 (d, *J* = 8.5 Hz, 2H), 7.21 (dd, *J* = 8.5, 2.2 Hz, 4H), 7.03 (s, 2H), 3.91 (s, 3H), 3.91 (s, 3H), 2.51 (s, 6H).  $\delta$  <sup>13</sup>C NMR (126 MHz; CDCl<sub>3</sub>)  $\delta$  154.1 (C), 154.0 (C), 139.8 (C), 139.7 (C), 132.1 (CH), 132.0 (CH), 131.8 (CH), 131.6 (CH), 126.0 (CH), 125.9 (CH), 123.4 (C), 123.1 (C), 119.6 (C), 119.4 (C), 115.7 (CH), 113.8 (C), 113.2 (C), 95.2 (C), 94.9 (C), 91.4 (C), 89.4 (C), 87.7 (C), 85.9 (C), 56.6 (CH<sub>3</sub>), 15.5 (CH<sub>3</sub>). HRMS (ES): *m/z* [M+H]<sup>+</sup> calcd for C<sub>34</sub>H<sub>27</sub>O<sub>2</sub>S<sub>2</sub>: 531.1452; found: 531.1442.

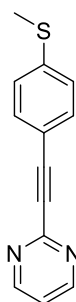
**Compound OPE3/S-pym.**



**OPE3/S-pym**

A solution of **S5** (408 mg, 1.64 mmol) dissolved in 6 mL of THF was added dropwise to a carefully degassed solution of Pd(CH<sub>3</sub>CN)<sub>2</sub>Cl<sub>2</sub> (21 mg, 0.08 mmol), CuI (16 mg, 0.08 mmol), tBu<sub>3</sub>P·HBF<sub>4</sub> (47 mg, 0.16 mmol) and 5-bromopyrimidine (261 mg, 1.64 mmol) in 5 mL of *i*Pr<sub>2</sub>NH. Afterwards, the reaction was stirred at room temperature under argon atmosphere during 24 h. The mixture was then diluted with CH<sub>2</sub>Cl<sub>2</sub> and washed with saturated aq NH<sub>4</sub>Cl solution. The organic layer was dried over anhydrous Na<sub>2</sub>SO<sub>4</sub> and the solvent removed under reduced pressure. The residue was purified by flash chromatography (SiO<sub>2</sub>, EtOAc/Hexane 1:9) and then CH<sub>2</sub>Cl<sub>2</sub> to give **OPE3/S-pym** (250 mg, 47%) as a yellow solid.  $\delta$  <sup>1</sup>H NMR (400 MHz; CD<sub>2</sub>Cl<sub>2</sub>) 9.12 (s, 1H), 8.86 (s, 2H), 7.55 (d, *J* = 2.0 Hz, 4H), 7.46 (d, *J* = 8.4 Hz, 2H), 7.24 (d, *J* = 8.4 Hz, 2H), 2.51 (s, 3H).  $\delta$  <sup>13</sup>C NMR (101 MHz; CD<sub>2</sub>Cl<sub>2</sub>) 159.2 (CH), 157.4 (CH), 140.9 (C), 132.4 (CH), 132.3 (CH), 132.1 (CH), 126.3 (CH), 124.9 (C), 122.1 (C), 120.2 (C), 119.4 (C), 96.0 (C), 92.2 (C), 89.3 (C), 84.7 (C), 15.6 (CH<sub>3</sub>). HRMS (ES): *m/z* [M+H]<sup>+</sup> calcd for C<sub>21</sub>H<sub>15</sub>N<sub>2</sub>S: 327.0956; found: 327.0950.

**Compound OPE2/S-pym.**

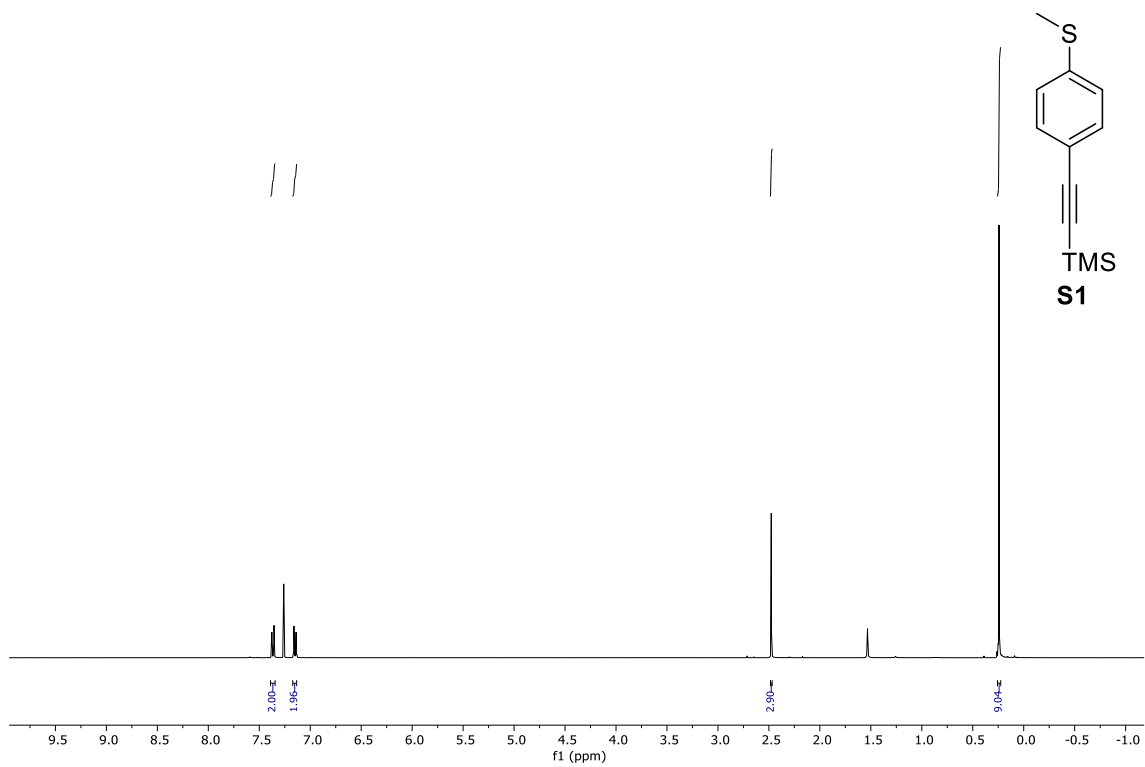


**OPE2/S-pym**

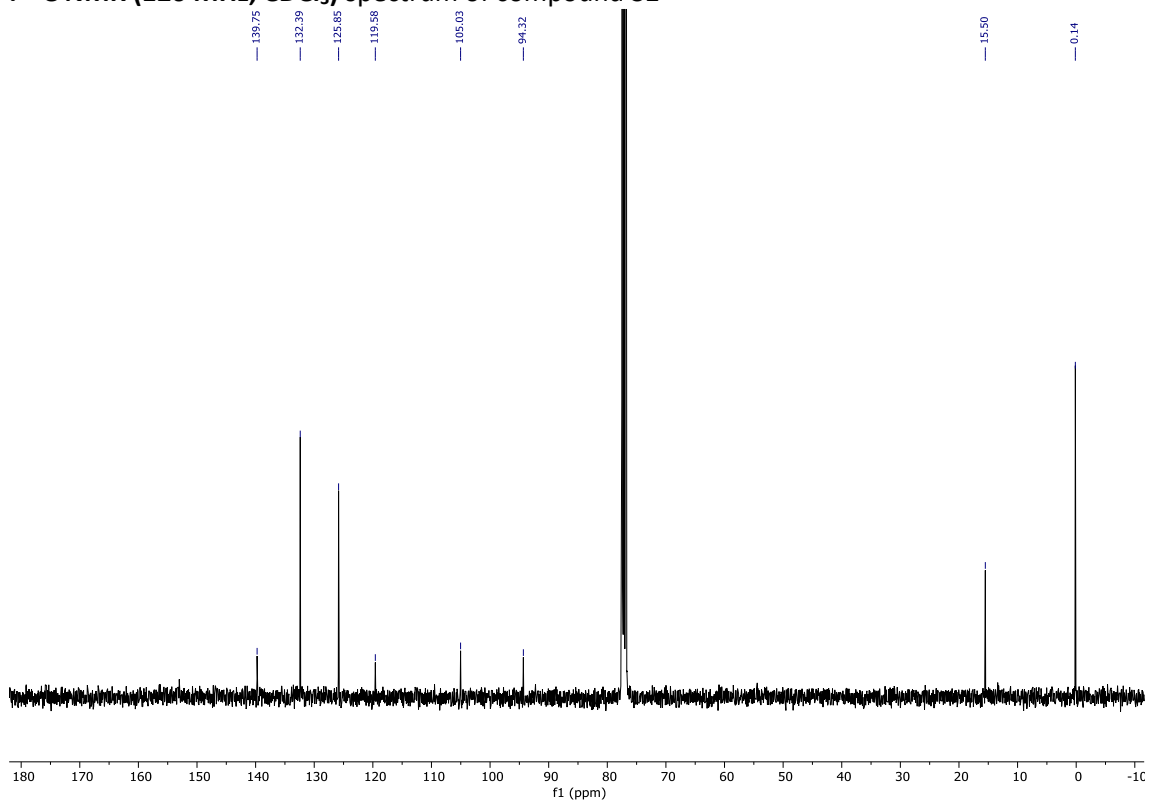
A solution of **S2** (400 mg, 2.72 mmol) dissolved in 5 mL of THF was added dropwise to a carefully degassed solution of Pd(CH<sub>3</sub>CN)<sub>2</sub>Cl<sub>2</sub> (35 mg, 0.14 mmol), CuI (26 mg, 0.14 mmol), tBu<sub>3</sub>P·HBF<sub>4</sub> (79 mg, 0.27 mmol) and 2-bromopyrimidine (432 mg, 2.72 mmol) in 5 mL of *i*Pr<sub>2</sub>NH. Afterwards, the reaction was stirred at room temperature under argon atmosphere during 24 h. The mixture was then diluted with EtOAc and washed with saturated aq NH<sub>4</sub>Cl solution. The organic layer was dried over anhydrous Na<sub>2</sub>SO<sub>4</sub> and the solvent removed under reduced pressure. The residue was purified by flash chromatography (SiO<sub>2</sub>, EtOAc/Hexane 1:9) and then EtOAc to give **OPE2/S-pym** (120 mg, 20%) as a yellow solid.  $\delta$  <sup>1</sup>H NMR (400 MHz, CD<sub>2</sub>Cl<sub>2</sub>) 8.72 (d, *J* = 5.0 Hz, 2H), 7.56 (d, *J* = 8.5 Hz, 2H), 7.27-7.21 (m, 3H), 2.51 (s, 3H).  $\delta$  <sup>13</sup>C NMR (101 MHz, CD<sub>2</sub>Cl<sub>2</sub>) 157.8 (CH), 153.8 (C), 142.4 (C), 133.2 (CH), 126.1 (CH), 120.2 (CH), 117.7 (C), 88.9 (C), 87.6 (C), 15.4 (CH<sub>3</sub>). HRMS (ES): *m/z* [M+H]<sup>+</sup> calcd for C<sub>13</sub>H<sub>11</sub>N<sub>2</sub>S: 227.0643; found: 227.0641.

## 2. $^1\text{H}$ and $^{13}\text{C}$ NMR spectra of new compounds

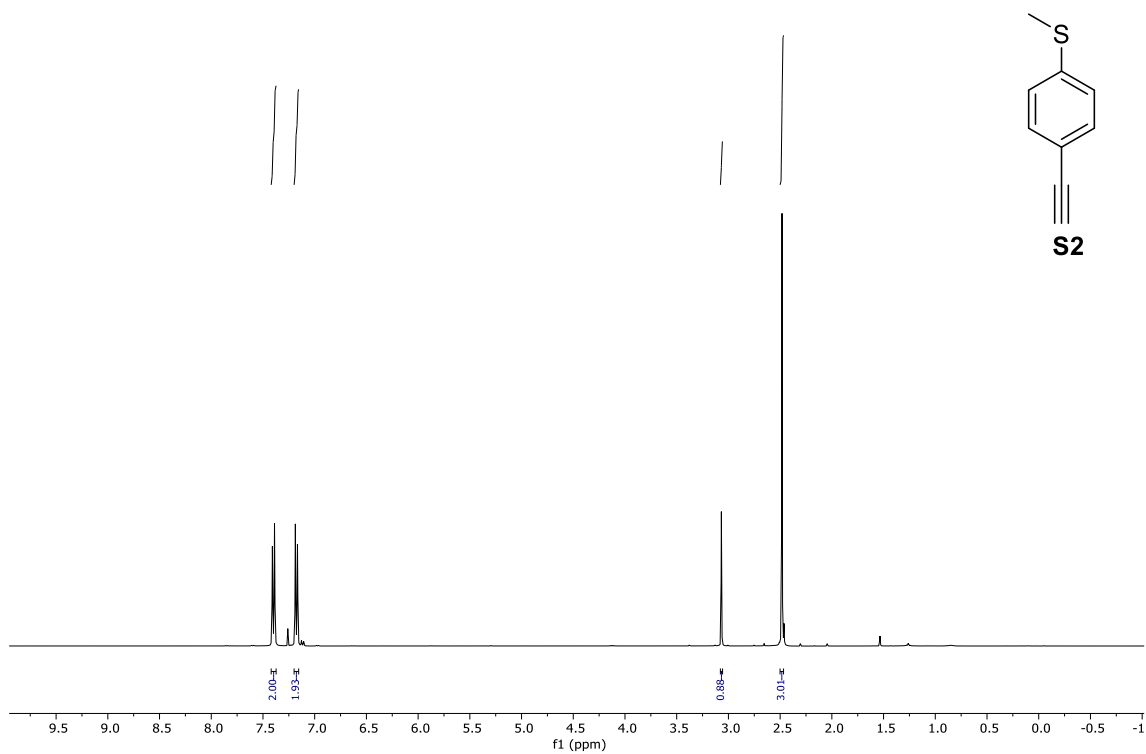
.  $^1\text{H}$  NMR (400 MHz,  $\text{CDCl}_3$ ) spectrum of compound S1



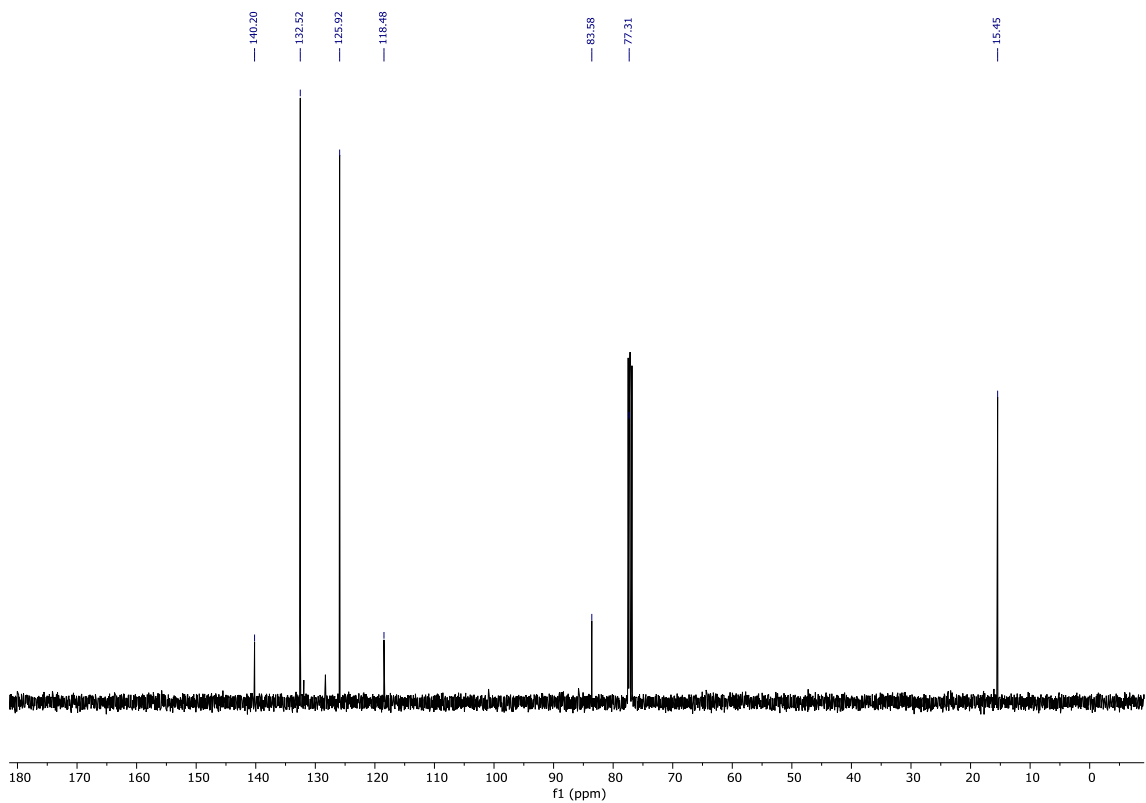
.  $^{13}\text{C}$  NMR (126 MHz,  $\text{CDCl}_3$ ) spectrum of compound S1



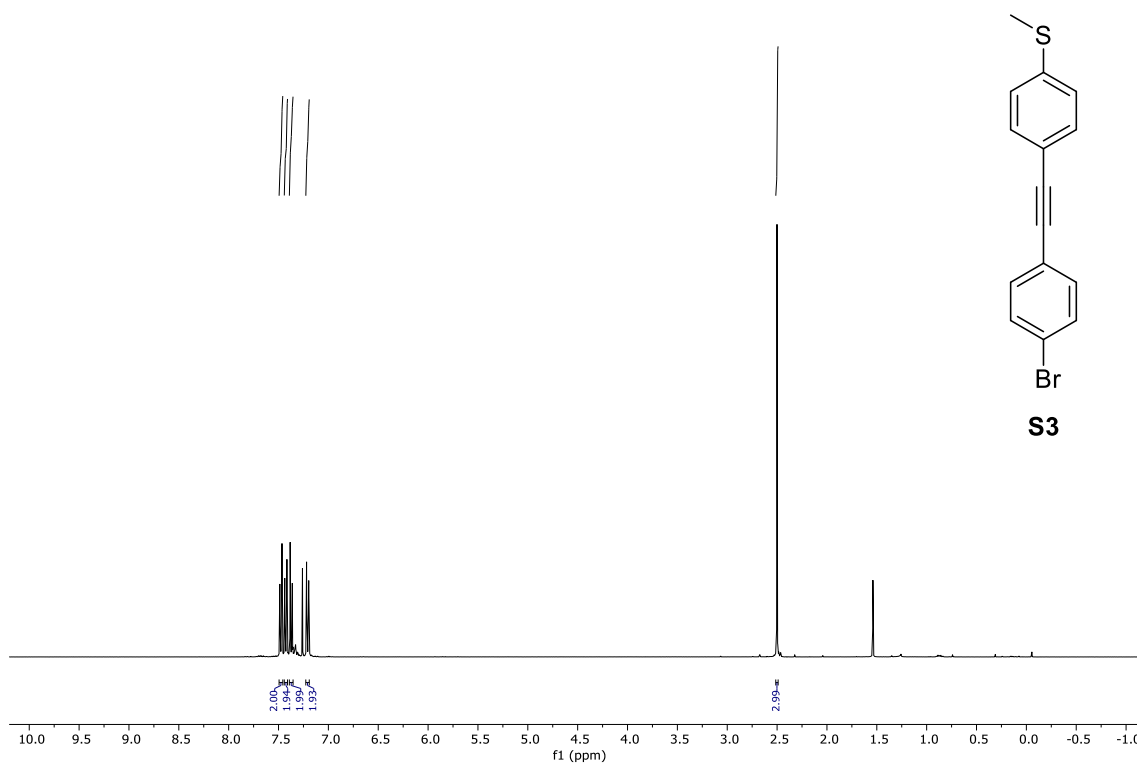
**<sup>1</sup>H NMR (400 MHz, CDCl<sub>3</sub>) spectrum of compound S2**



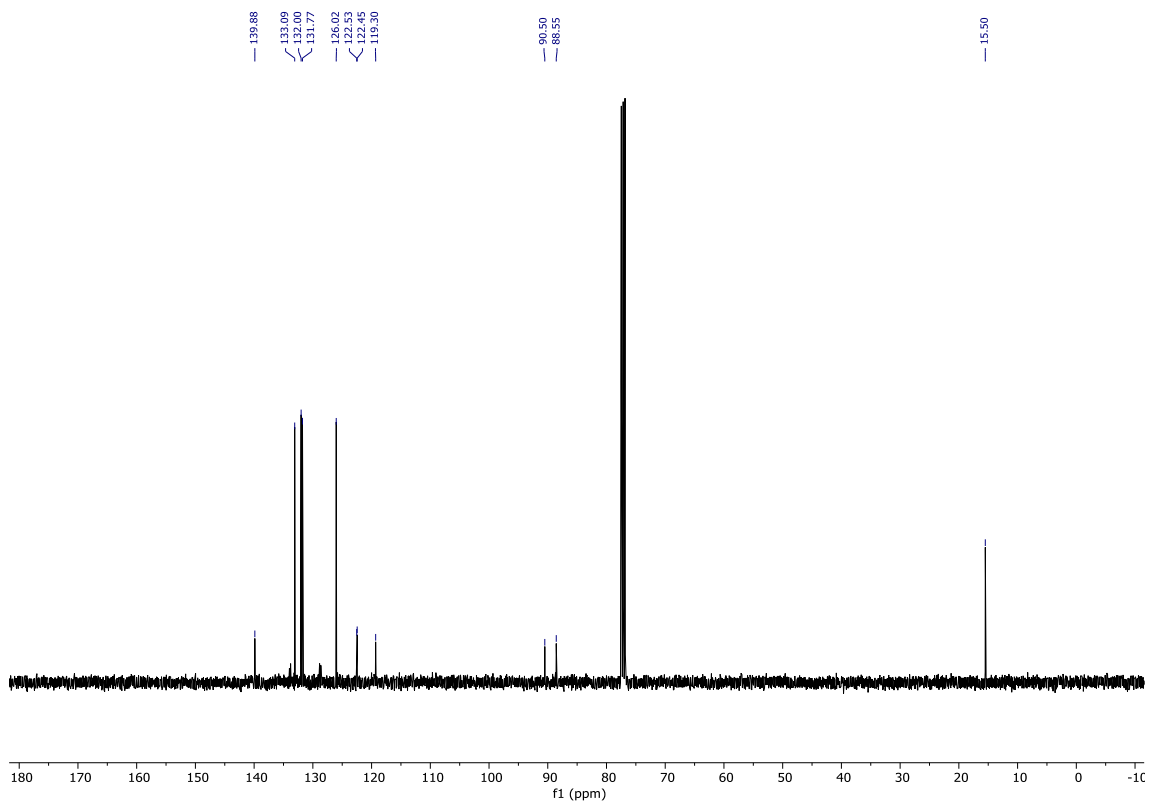
**<sup>13</sup>C NMR (126 MHz, CDCl<sub>3</sub>) spectrum of compound S2**



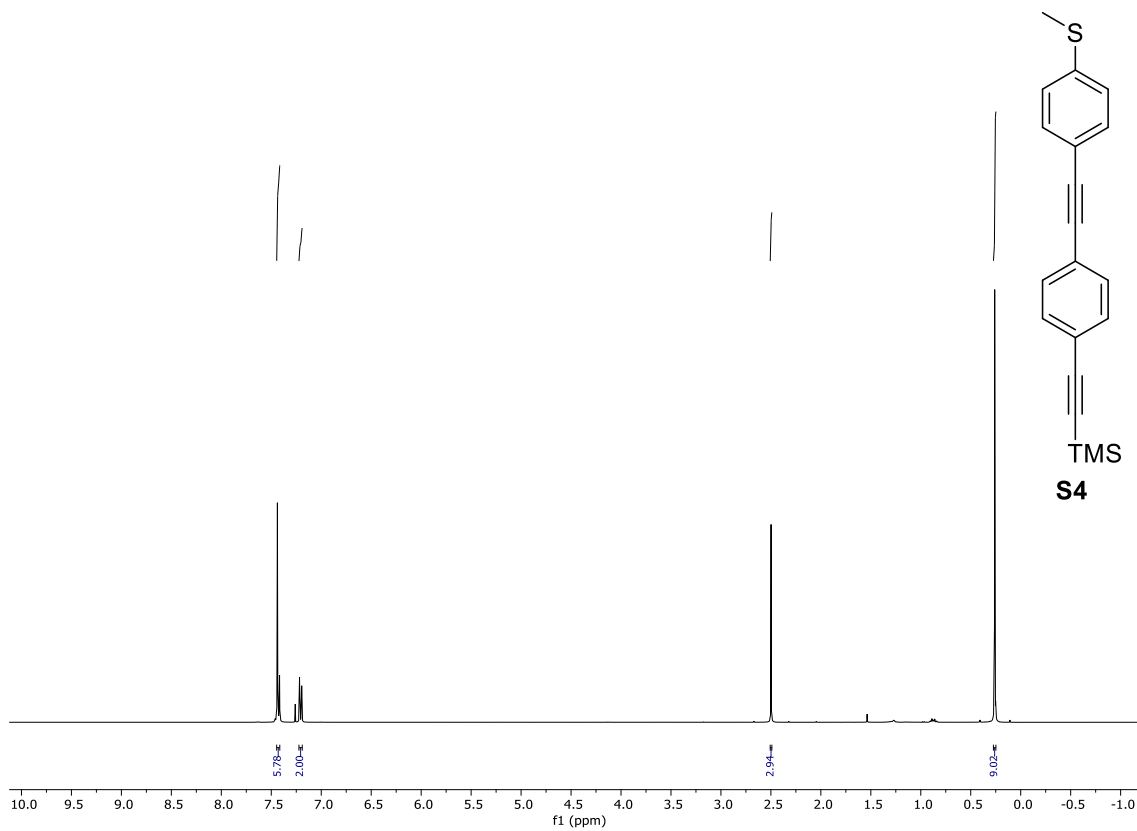
**<sup>1</sup>H NMR (400 MHz, CDCl<sub>3</sub>) spectrum of compound S3**



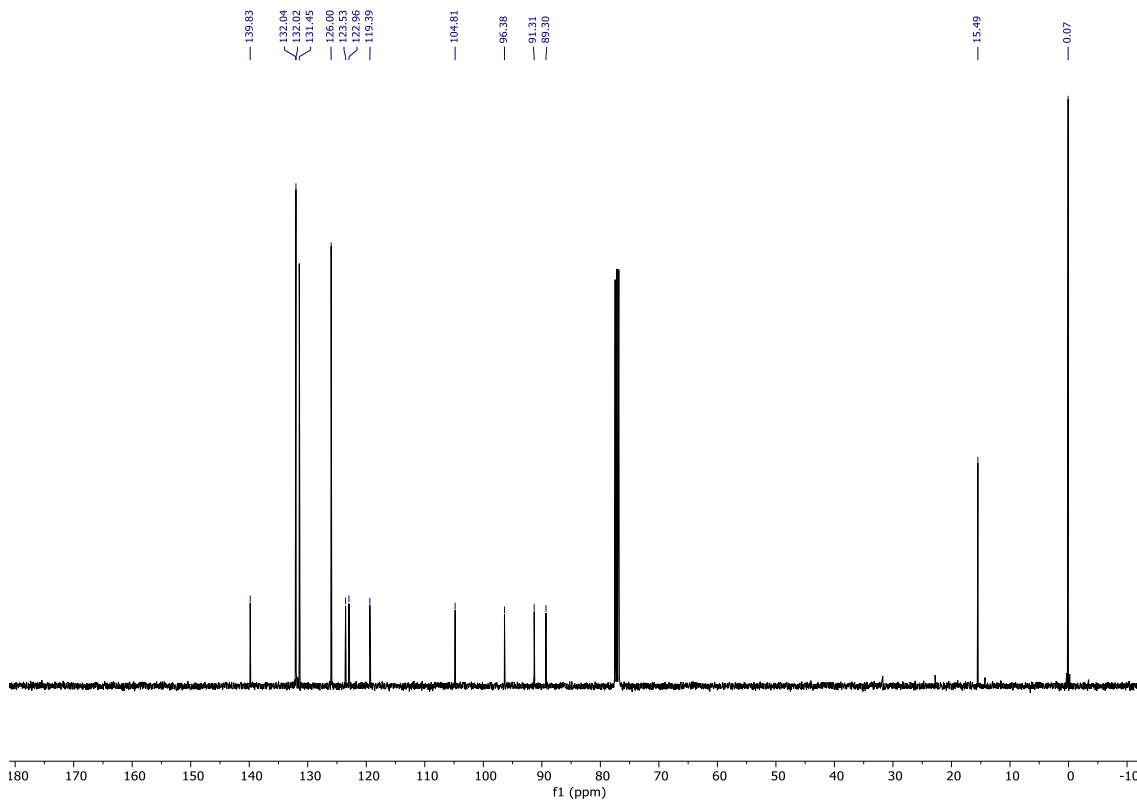
**<sup>13</sup>C NMR (126 MHz, CDCl<sub>3</sub>) spectrum of compound S3**



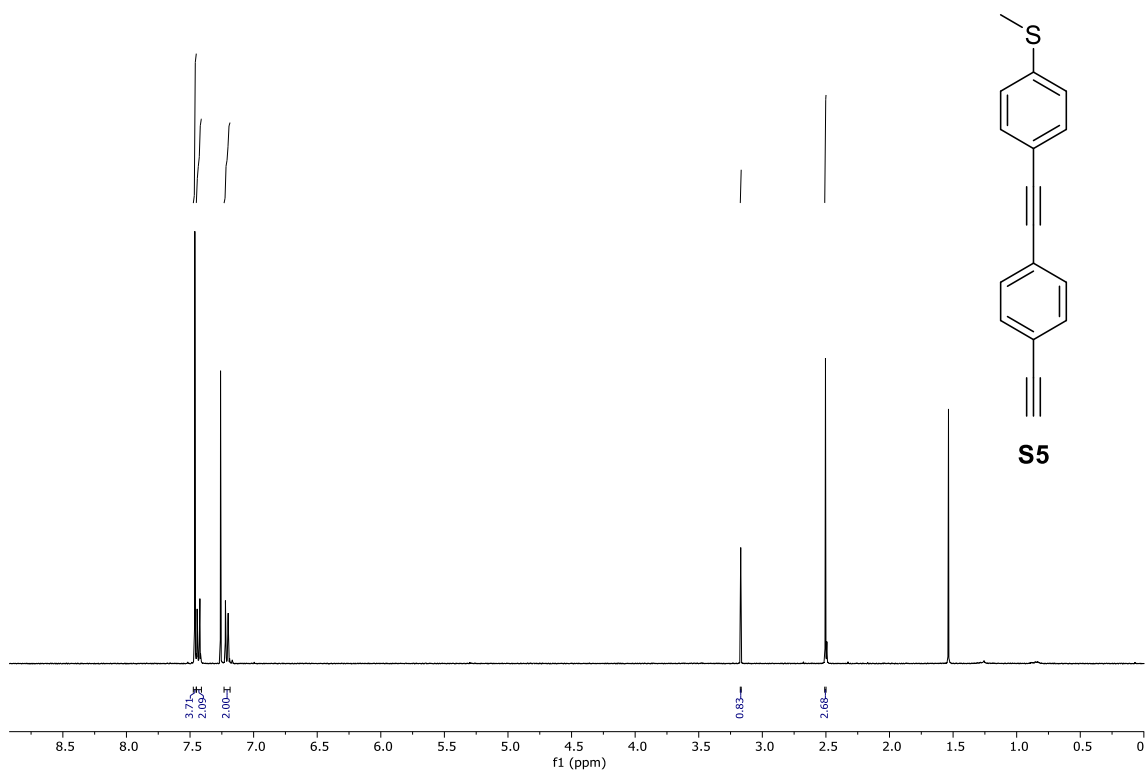
**<sup>1</sup>H NMR (400 MHz, CDCl<sub>3</sub>) spectrum of compound S4**



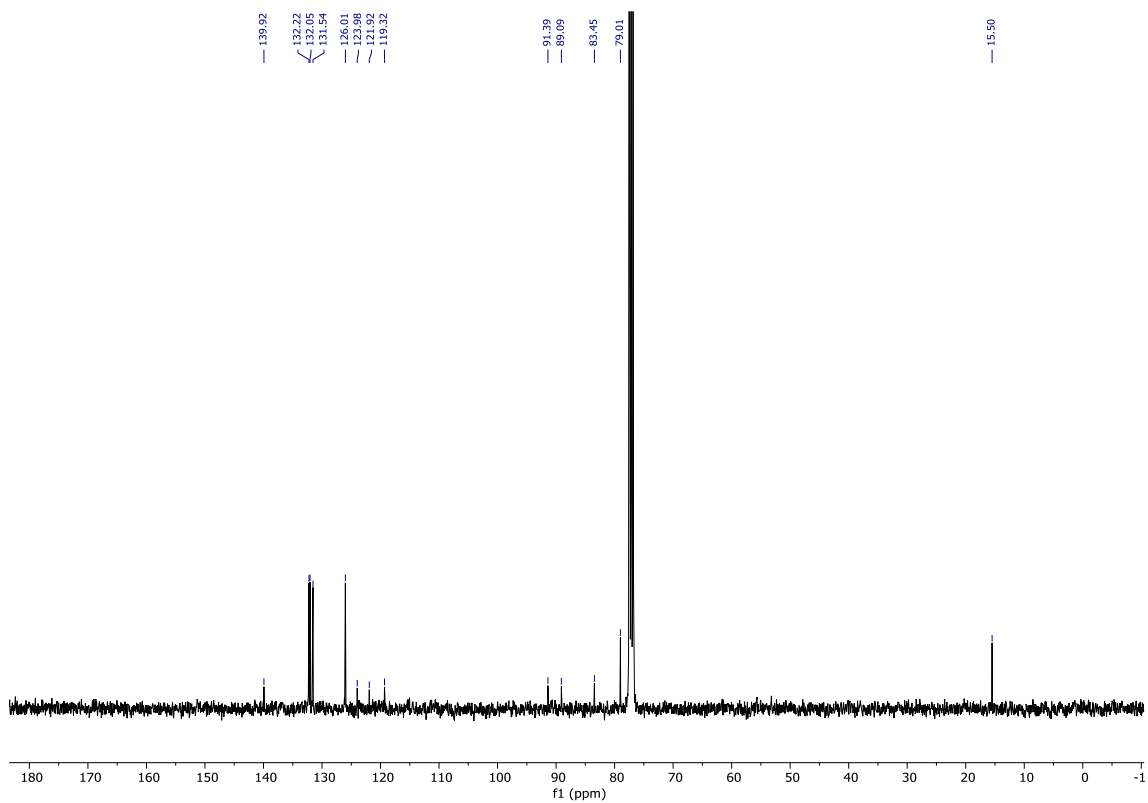
**<sup>13</sup>C NMR (126 MHz, CDCl<sub>3</sub>) spectrum of compound S4**



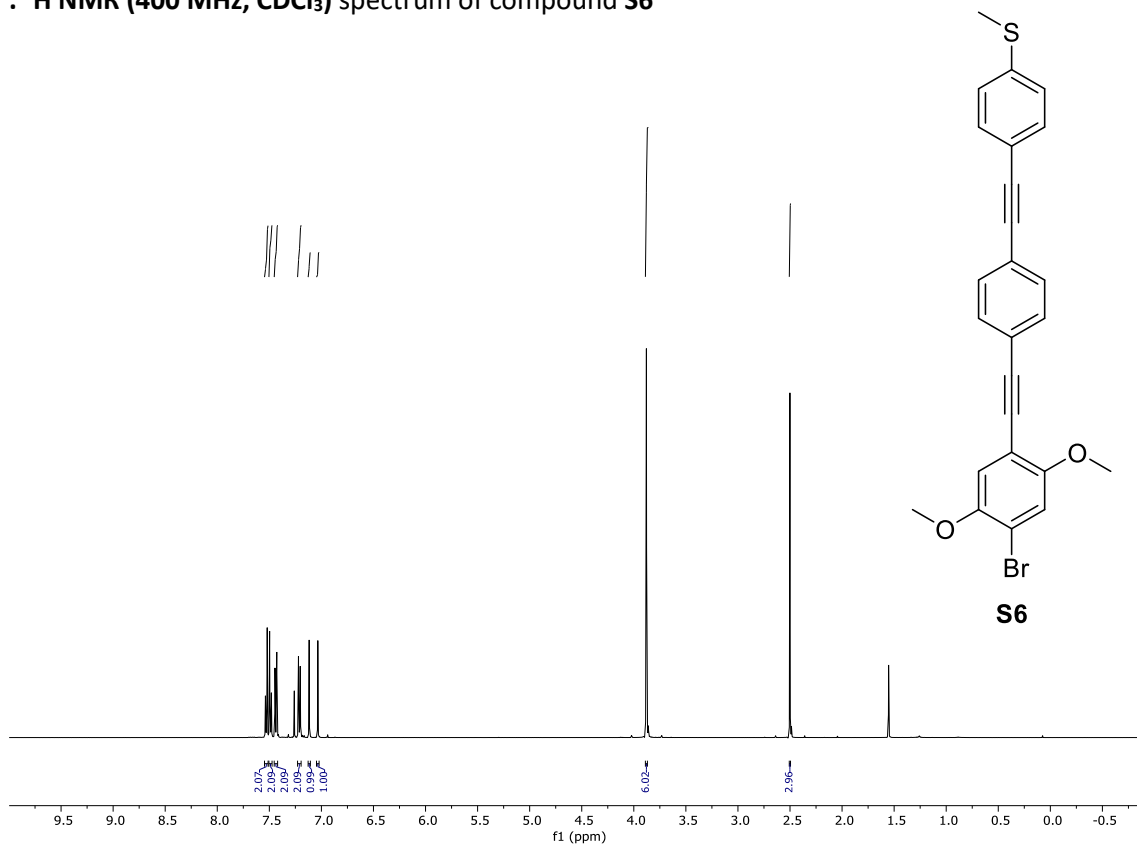
**<sup>1</sup>H NMR (400 MHz, CDCl<sub>3</sub>) spectrum of compound S5**



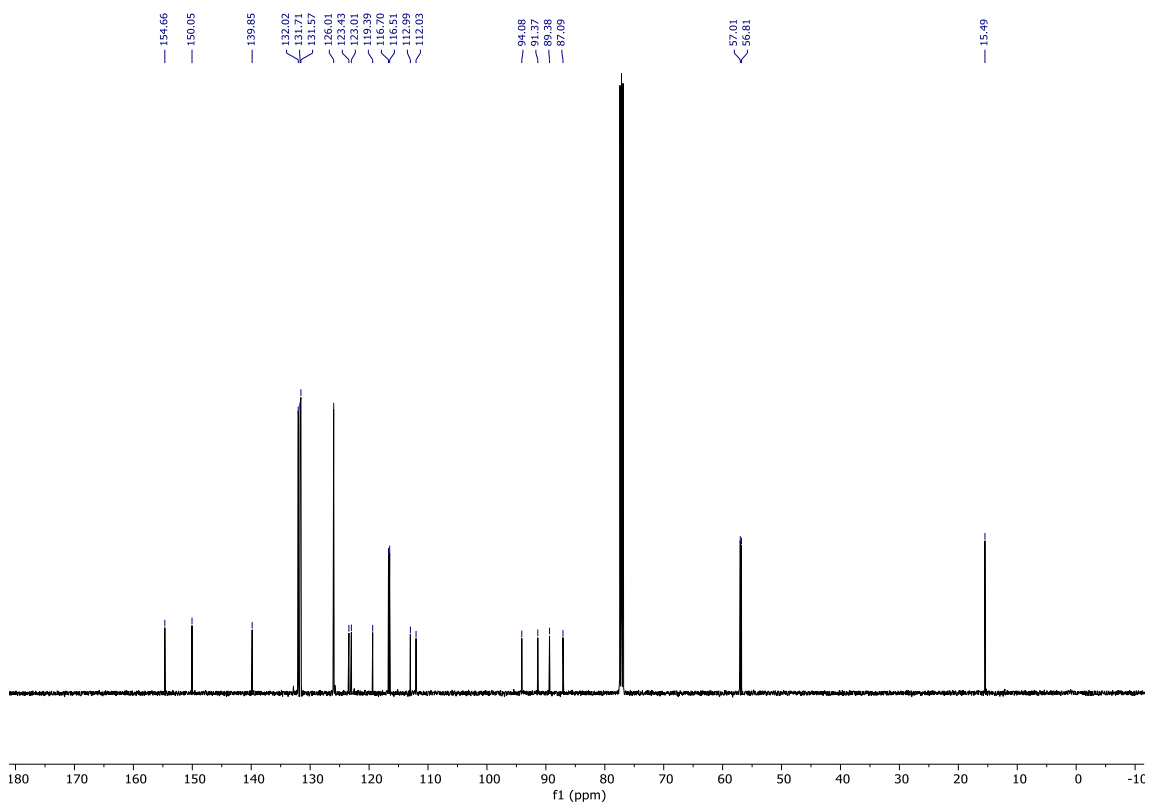
**<sup>13</sup>C NMR (126 MHz, CDCl<sub>3</sub>) spectrum of compound S5**



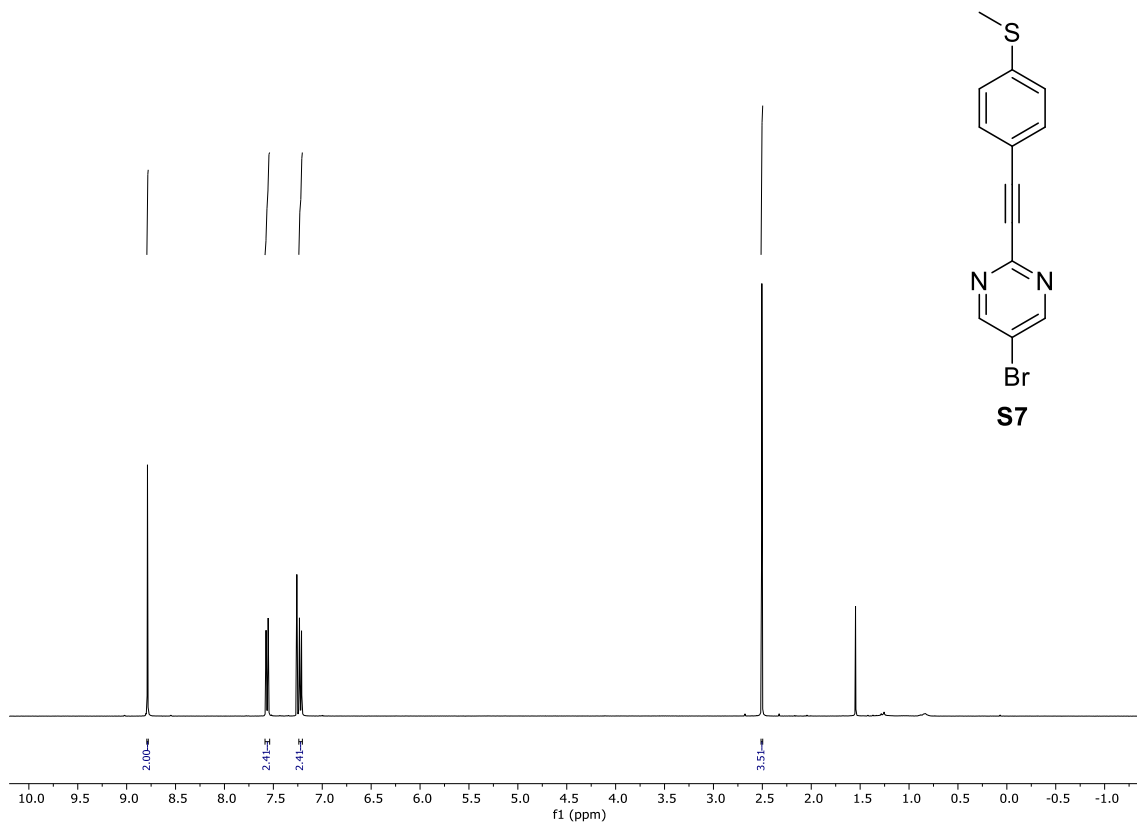
**<sup>1</sup>H NMR (400 MHz, CDCl<sub>3</sub>) spectrum of compound S6**



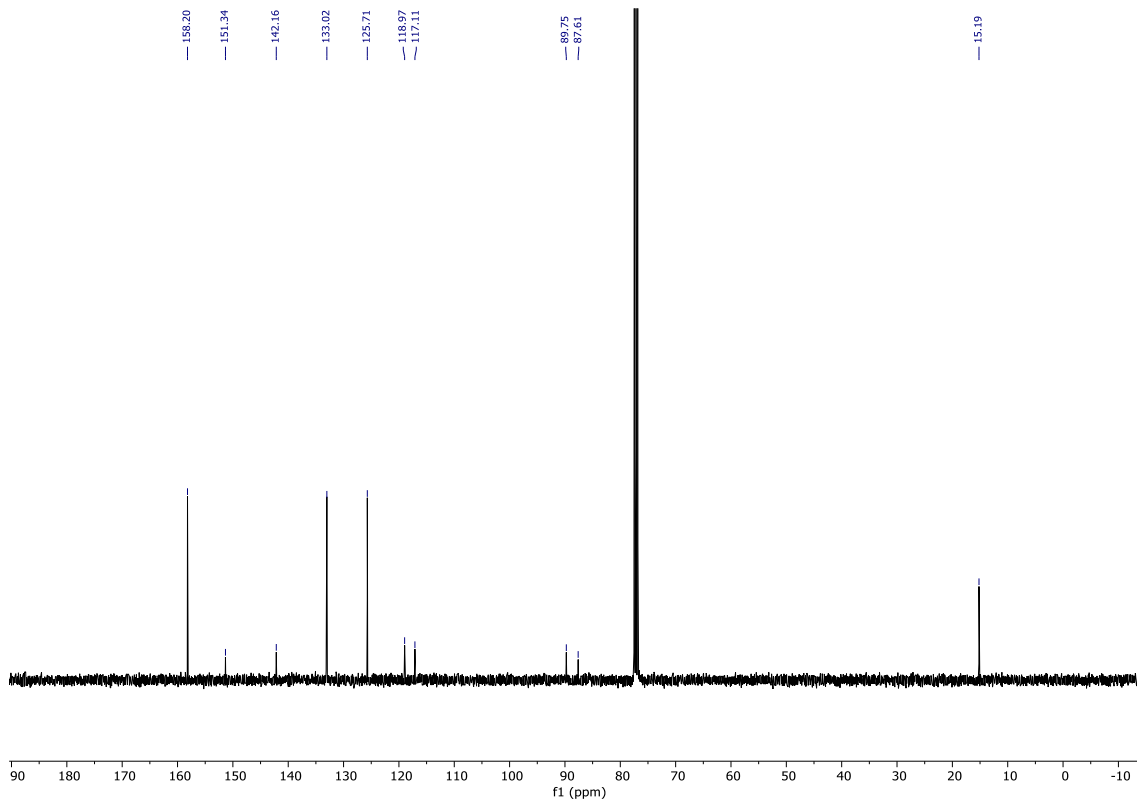
**<sup>13</sup>C NMR (126 MHz, CDCl<sub>3</sub>) spectrum of compound S6**



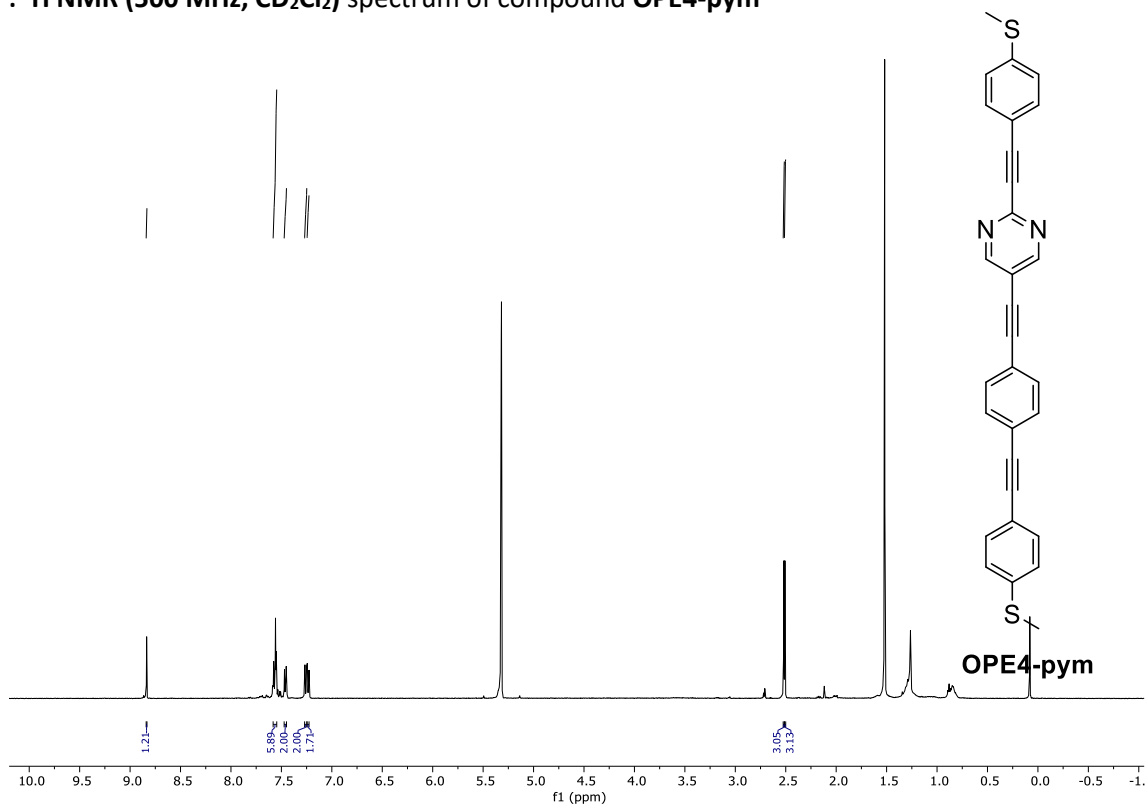
**<sup>1</sup>H NMR (400 MHz, CDCl<sub>3</sub>) spectrum of compound S7**



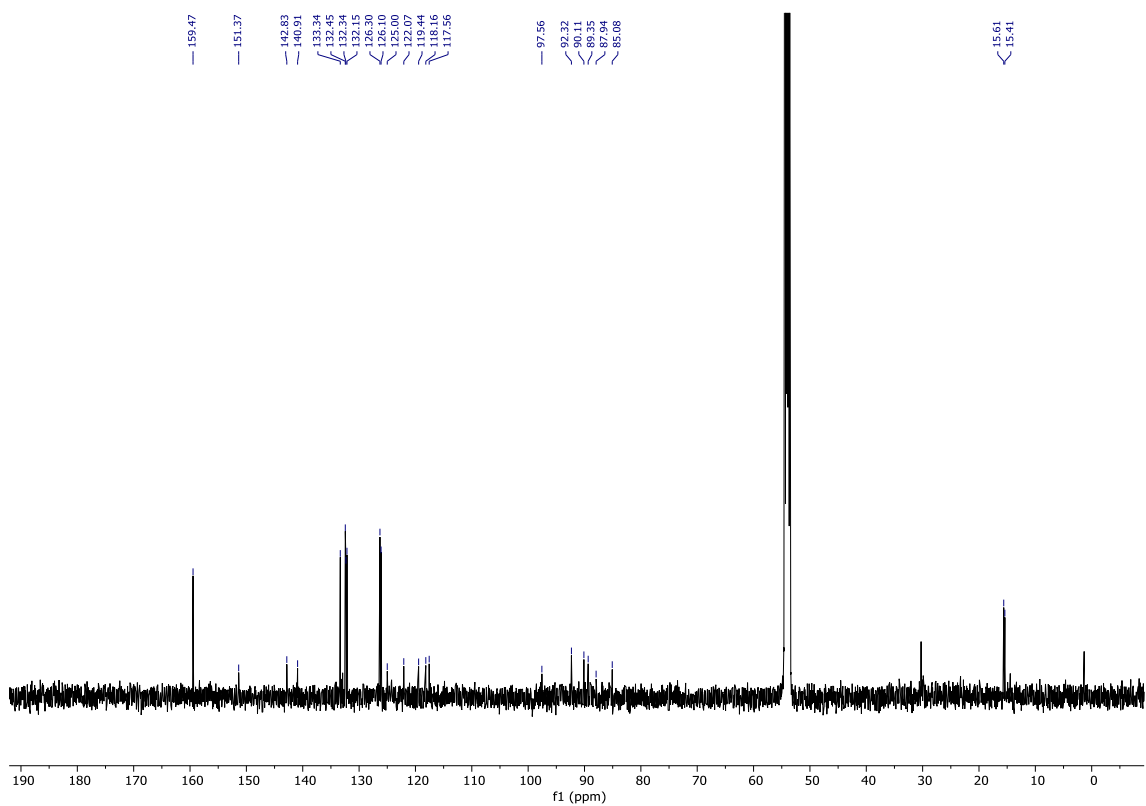
**<sup>13</sup>C NMR (126 MHz, CDCl<sub>3</sub>) spectrum of compound S7**



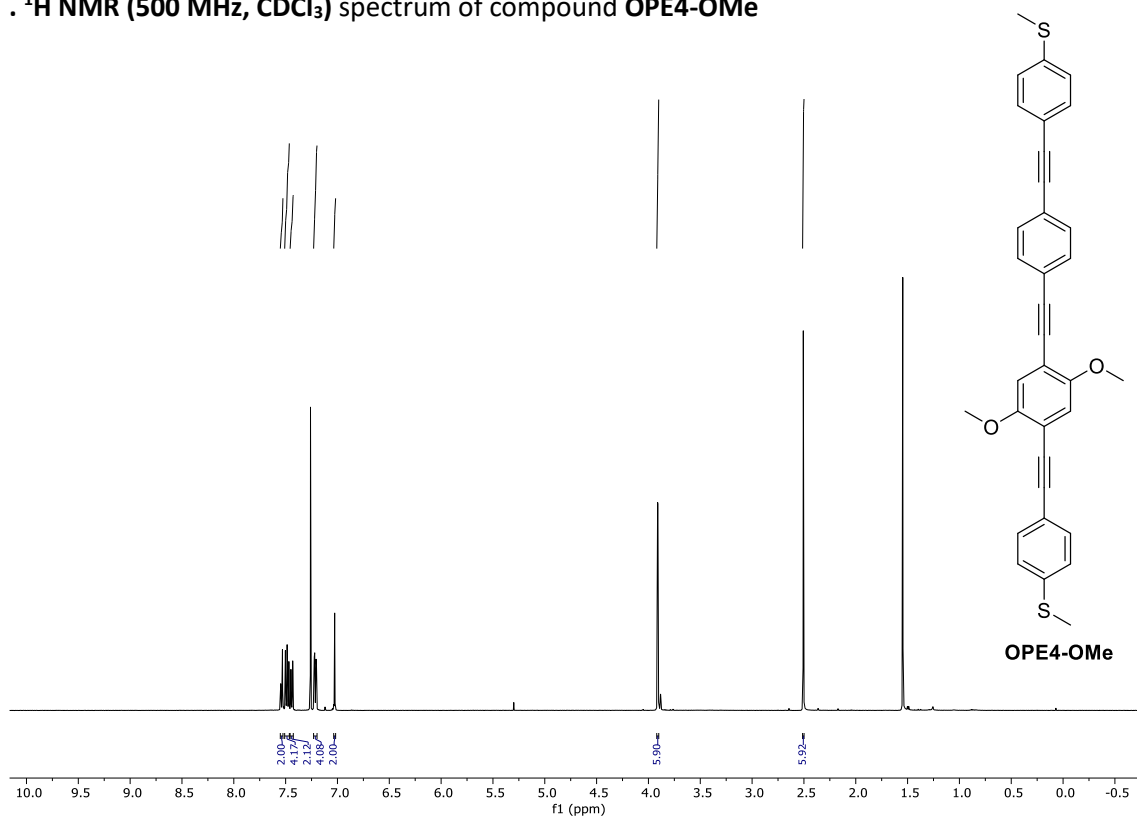
**<sup>1</sup>H NMR (500 MHz, CD<sub>2</sub>Cl<sub>2</sub>) spectrum of compound OPE4-pym**



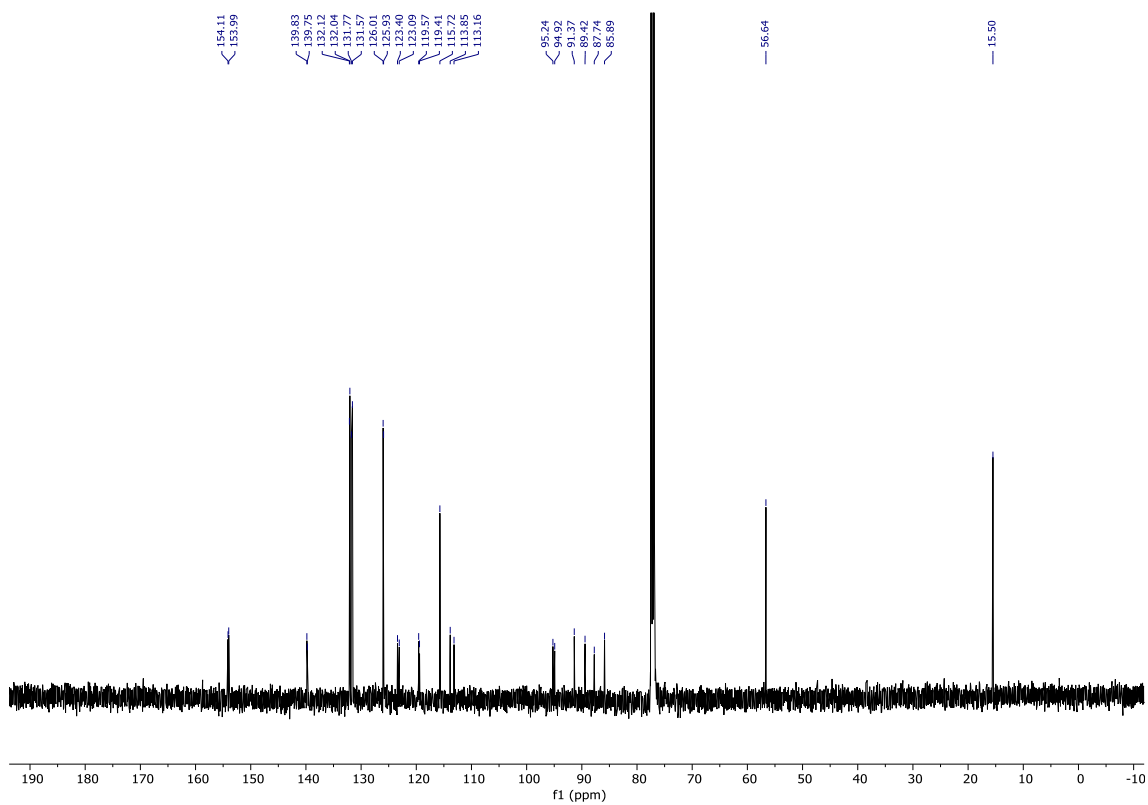
**<sup>13</sup>C NMR (126 MHz, CD<sub>2</sub>Cl<sub>2</sub>) spectrum of compound OPE4-pym**



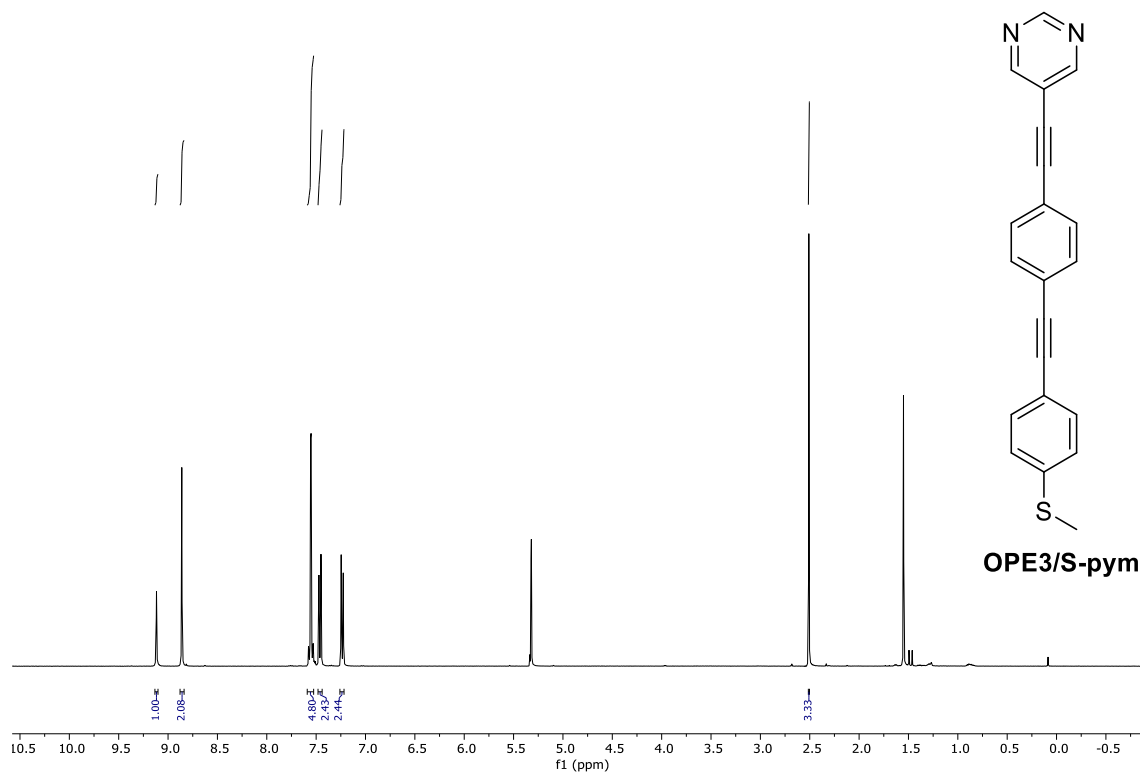
**<sup>1</sup>H NMR (500 MHz, CDCl<sub>3</sub>) spectrum of compound OPE4-OMe**



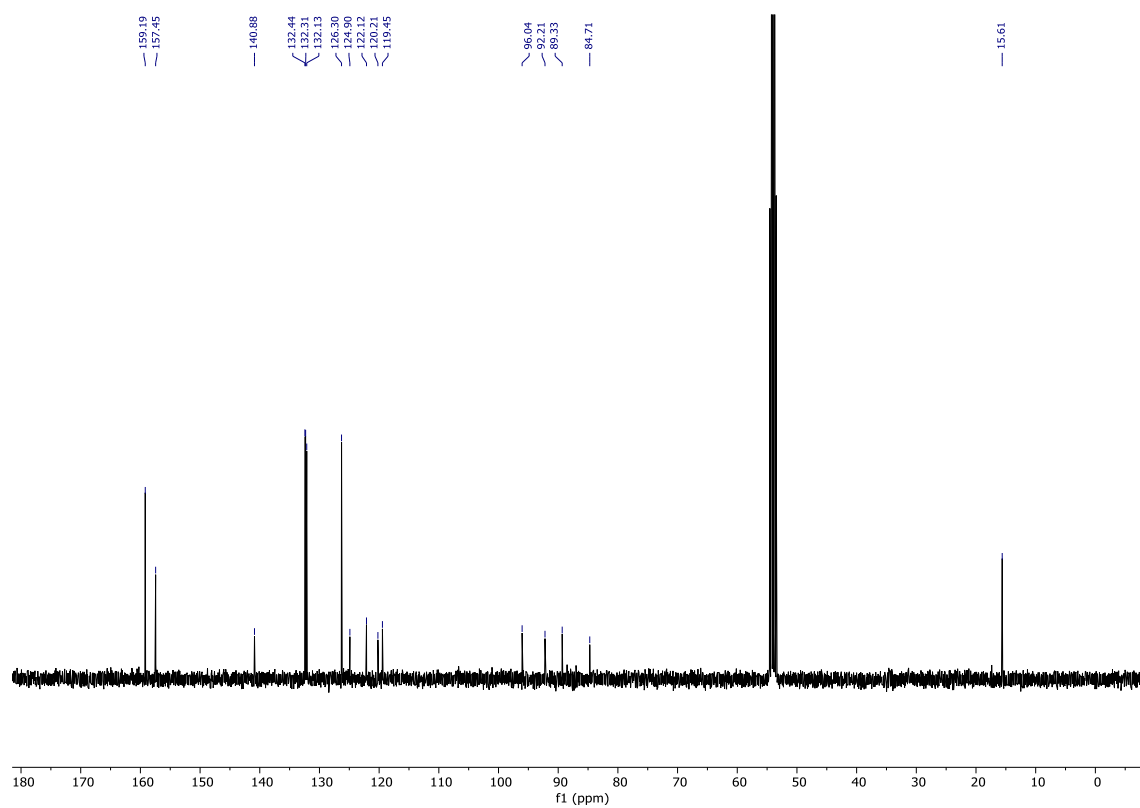
**<sup>13</sup>C NMR (126 MHz, CDCl<sub>3</sub>) spectrum of compound OPE4-OMe**



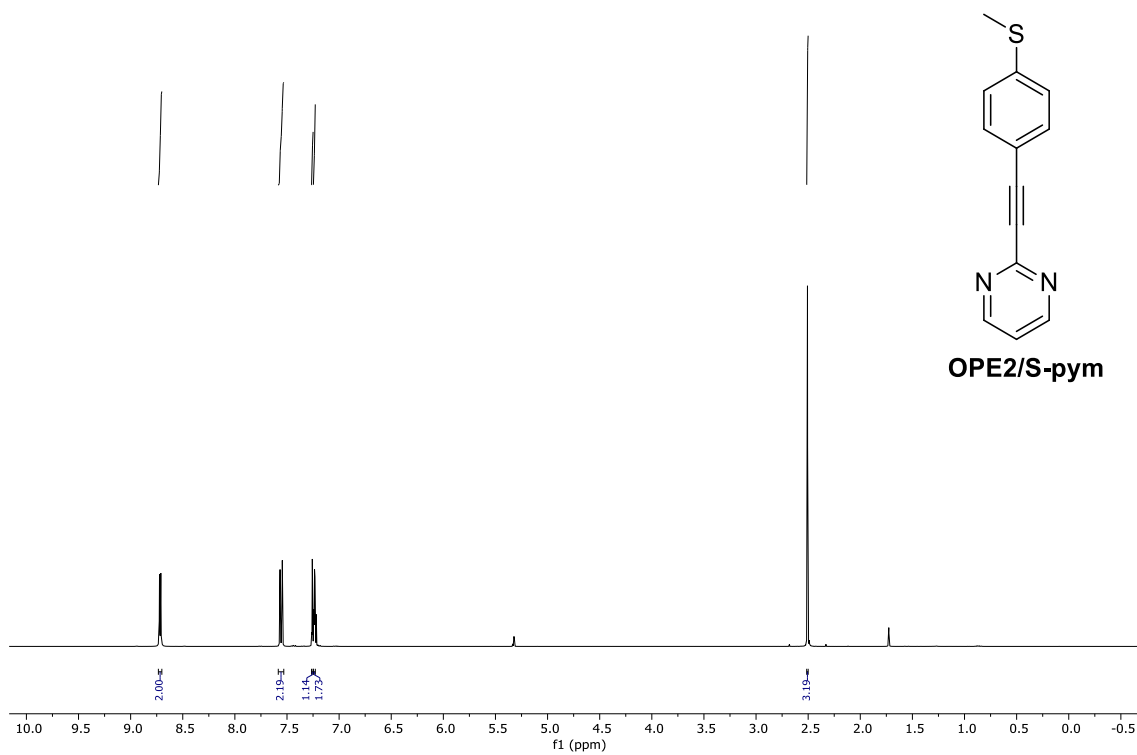
**<sup>1</sup>H NMR (400 MHz, CD<sub>2</sub>Cl<sub>2</sub>) spectrum of compound OPE3/S-pym**



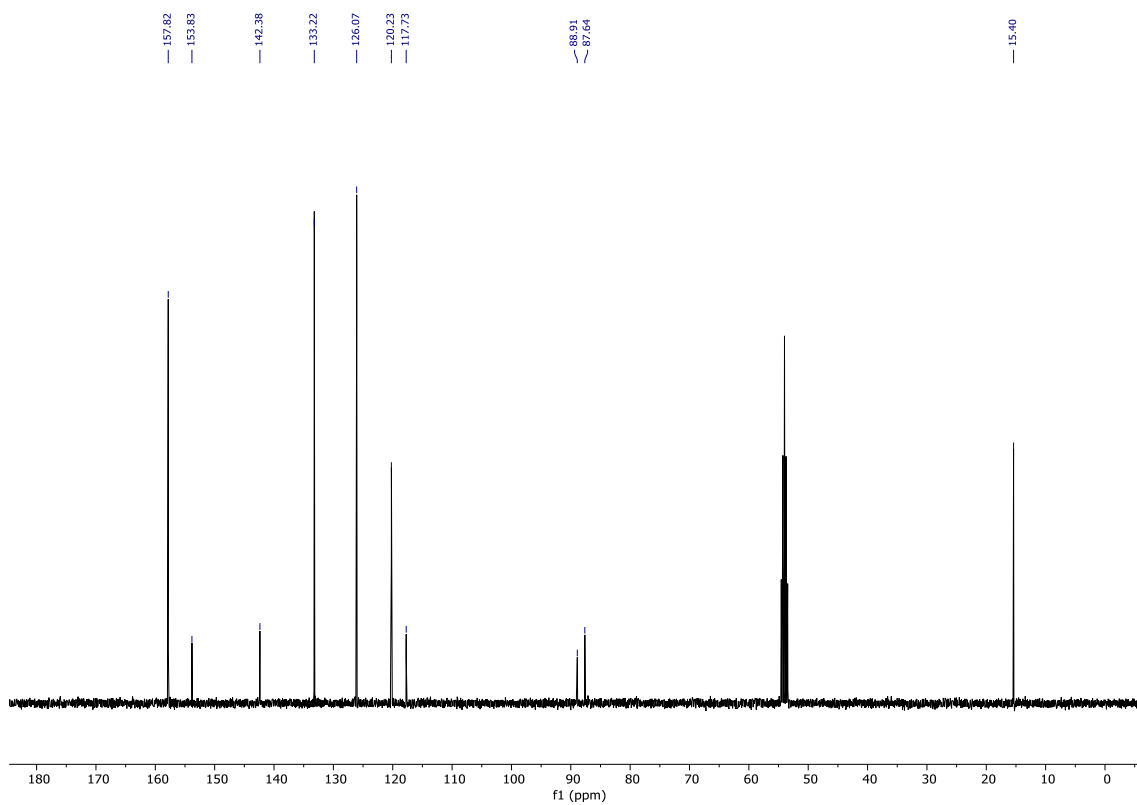
**<sup>13</sup>C NMR (126 MHz, CD<sub>2</sub>Cl<sub>2</sub>) spectrum of compound OPE3/S-pym**



**<sup>1</sup>H NMR (400 MHz, CD<sub>2</sub>Cl<sub>2</sub>) spectrum of compound OPE2/S-pym**



**<sup>13</sup>C NMR (126 MHz, CD<sub>2</sub>Cl<sub>2</sub>) spectrum of compound OPE2/S-pym**



### **3. BREAK-JUNCTION EXPERIMENTS**

The experiments are based in a push-pull process between the STM electrodes. After pushing the STM tip and substrate into contact, the tip is pulled upwards, and the current between both electrodes decreases in a stepwise fashion. These steps correspond to quantized units of  $G_0=2e^2/h$ , which means that the metallic contact size is decreasing in only one Au atom from one step to the next. A last plateau at  $G_0$  is formed when the contact between the electrodes consists in just one gold atom. New plateaus appearing at  $G < G_0$ , indicate that one or a few molecular bridges have been formed between the electrodes and the conductance value of those plateaus is assigned to the molecular junction conductance.

#### Data analysis

Several rounds of thousands of  $G$ - $z$  traces were collected for each compound, changing to new tips, substrates or even different product batches in order to ensure the reproducibility of results.

The total of  $G$ - $z$  traces recorded for each compound were submitted to an automatic algorithm able to separate the traces displaying molecular signals, or plateau regions, from those displaying an exponential conductance decay due to tunneling current. The criterion for considering a trace containing plateau was that a change in conductance of  $\Delta \log(G/G_0) = x$  needs to be related with a displacement ( $\Delta z$ ) larger than  $y$  nm. Importantly, the values of  $x$  and  $y$  were modified according to the requirements of each compound. We built 1D and 2D conductance histograms from all these traces displaying plateaus. 1D histograms were built by accumulating the number of points  $N_{\text{points}}$  measured in fixed  $\log(G/G_0)$  intervals ( $\Delta \log(G/G_0)$ ). The  $y$ -axis in these histograms is normalized, as

$$N_{\text{norm}} = N_{\text{points}} / (N_{\text{curves}} \cdot v_p \cdot \Delta \log(G/G_0))$$

where  $N_{\text{curves}}$  is the total number of  $G$ - $z$  traces included in the histogram, and  $v_p$  is the number of points recorded per unit of length in  $z$ .<sup>2</sup> With this normalization,  $N_{\text{norm}}$  is the

---

<sup>2</sup> C. R. Arroyo, E. Leary, A. Castellanos-Gomez, G. Rubio Bollinger, M. T. Gonzalez and N. Agrait, *J. Am. Chem. Soc.*, 2011, **133**, 14313.

inverse of the typical  $\log(G/G_0)$  vs  $z$  curve, that tells us the distance  $z$  that we would need to move to produce a variation of 1 order of magnitude in conductance  $G$  at each particular point. Therefore, it has units of nanometers per order of magnitude that we abbreviate to nm/order-mag.

2D conductance-distance histograms provide a whole picture of the breaking process. After aligning the traces to the origin in  $z$  when  $G = 0.5 G_0$ , the histograms were built by accumulating the number of points  $N_{\text{points}}$  measured in fixed  $\log(G/G_0)$  and  $z$  intervals from the traces. In this case, a colour scale from green to brown was used for displaying the  $N_{\text{points}}$ , where green represents the  $G$ - $z$  intervals with fewer number of points and brown represents the  $G$ - $z$  intervals with higher number of points.

Figures S1 and S2 respectively show the 1D and 2D histograms of the measurement of **OPE4-pym** with and without plateaus in comparison with the blank experiment without molecules. In this case, the sample was exposed to the solvent (HPLC grade DCM) and then the  $G$  vs  $z$  curves were recorded in air in the same way as when testing the compounds of interest. A computer program was used to separate the traces with a plateau-like profile: those traces for which a displacement  $\Delta z$  larger than 0.1 nm is needed to produce a change in conductance of  $\Delta \log(G/G_0) = 0.1$  at any conductance below  $1 G_0$ . As shown in Figure S1, the routine also detects some traces showing plateaus in the blank experiment probably due to small amounts of contaminants on the substrate surface. However, their percentage is very low, and they occur over a wide range of conductance values, not producing prominent peaks in the histograms. On the other hand, when adding our compounds of interest, clear plateaus appear in at least 20 % of the traces that gave place to clear peaks in the histograms

The plateau length for each molecular signal was calculated as the variation of  $z$  ( $\Delta z$ ) needed to change the junction conductance from  $0.5 G_0$  to a conductance value just below the peak observed in the corresponding conductance histogram. The length of the plateaus was obtained for every individual trace and then plateau-length probability ( $p$ ) distributions were calculated using the data of all traces displaying plateaus. Examples of these distributions are shown in Figure 4 of the main text and in Figure S3. The comparison of this plateau-length probability distribution with the theoretical molecular length was carried out considering that the length of plateaus is

shorter than the theoretical length due to the electrode retraction after the gold contact breaks ( $\sim 0.4$  nm).

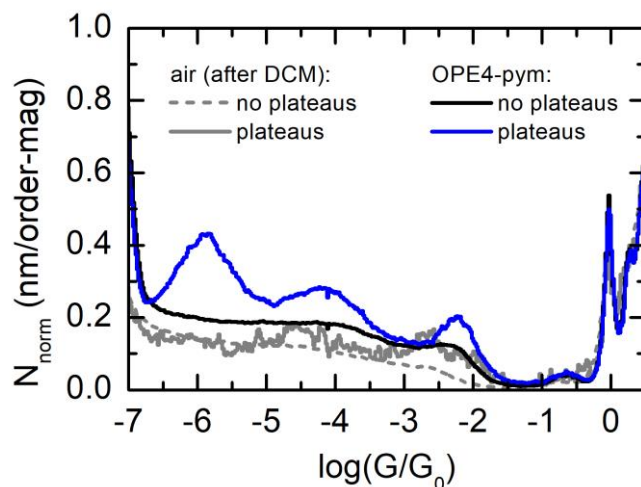


**Figure S1.** Conductance histograms recorded after exposing the substrate to a DCM solution of **OPE4-pym**, in comparison with the blank experiments without molecules. In both cases, the traces have been separated by a computer program in two groups according to their plateau-like profile (see text for details). For the case of air without molecules, the histogram of the traces with plateaus is very noisy due to the low number of traces (less than 200). Three clear peaks are observed in the histogram with plateau-like traces when **OPE-4pym** is added.

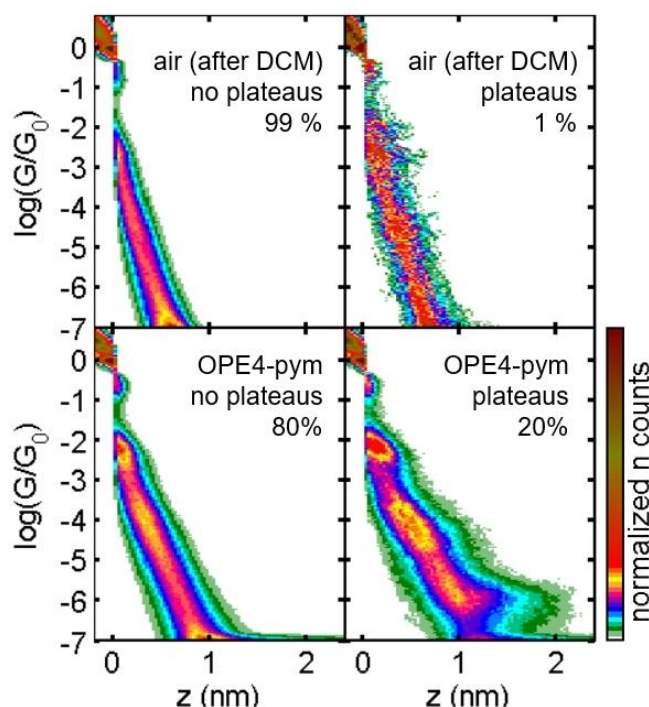


**Figure S2.** 2D histograms built with the same traces as in the 1D histograms of Figure S1. A percentage below 1 % of the total traces recorded in air (without molecules present) were detected by the program as plateau-like, while this percentage is about 20-26 % when **OPE4-pym** was present. In the latter case, clear conductance clouds of different length are observed in the resulting histogram.

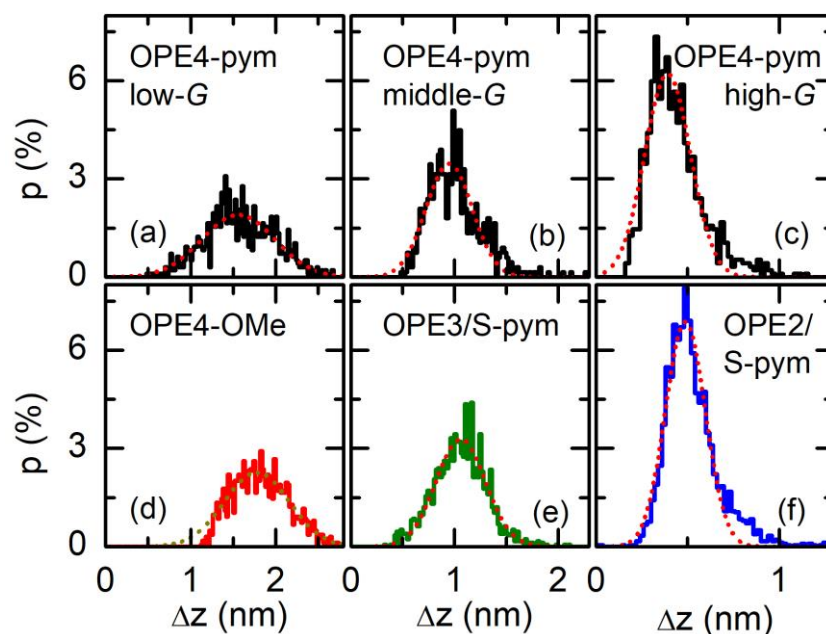


**Figure S3.** Plateau length distribution for the three conductance groups of **OPE4-pym** (a, b and c), together with their corresponding reference compound: **OPE4-OMe** (d), **OPE3/S-pym** (e) and **OPE2/S-pym** (f). The red dotted lines are fits of a gaussian curve to the distributions.

#### Additional Clustering Analysis

An additional unsupervised k-means clustering subdivision was used to analyze the molecular junction formation of the different compounds. We employed an algorithm similar to those described in literature,<sup>3</sup> using the 2D histograms of the individual  $G$ - $z$  traces previously selected as displaying plateaus. During the analysis of each compound, different numbers of blind subdivisions in the algorithm were explored, obtaining so many final subdivisions as the data required.

For **OPE4-pym**, three clear groups were identified, whose histograms are shown in Figure 3 of the main text and labelled as low- $G$ , middle- $G$  and high- $G$ . Figure S4 shows examples of individual  $G$  vs  $z$  traces in each of these groups. In our experiments, it was rare to find  $G$  vs  $z$  traces with plateaus in more than one conductance range, and these were not singled out by the clustering analysis. A visual inspection of the traces led us to estimate that only 2% of all the traces with plateaus displayed plateaus at high and

<sup>3</sup> (a) D. Cabosart, M. El Abassi, D. Stefani, R. Frisenda, M. Calame and H. S. J. van der Zant, *Appl. Phys. Lett.*, 2019, **114**, 143102. (b) M. El Abbassi, P. Zwick, A. Rates, D. Stefani, A. Prescimone, M. Mayor, H. S. J. van der Zant and D. Dulić, *Chem. Sci.*, 2019, **10**, 8299.

low  $G$  at the same time, and 3% displayed plateaus at middle and low  $G$ . Examples of these traces are shown in Figure S5. Traces with plateaus at high and middle  $G$  in the same trace could also be found, but these appeared in an even lower percentage, below 1% of all traces with plateaus.

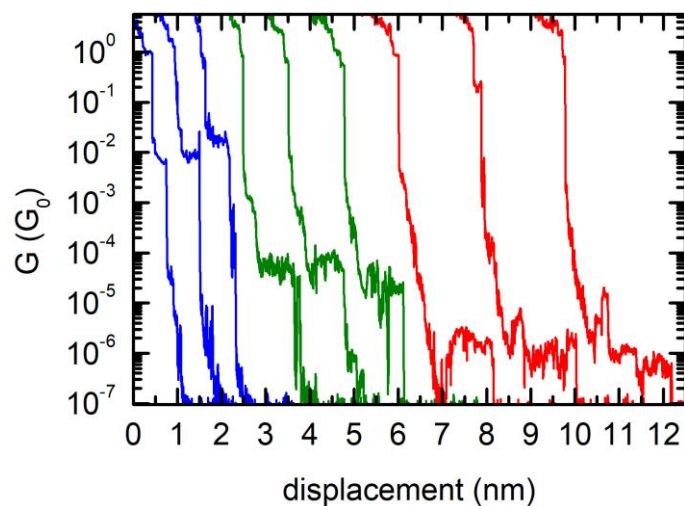


**Figure S4.** Examples of individual traces with plateaus at high  $G$  (blue), middle  $G$  (green) and low  $G$  (red) identified by an unsupervised k-means clustering analysis.

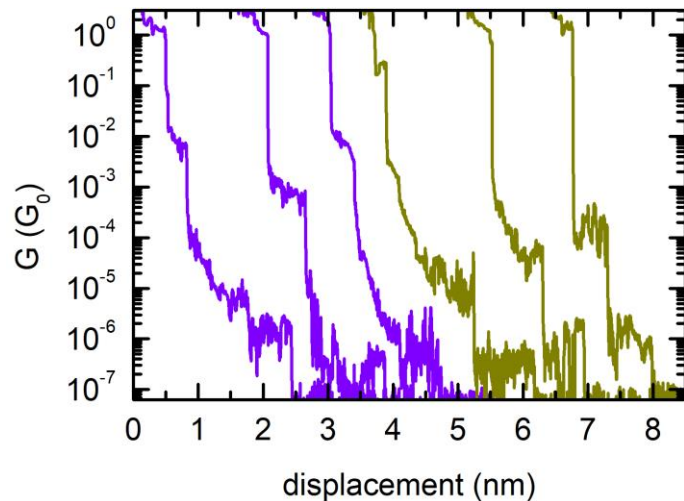


**Figure S5.** Examples of individual traces with simultaneous plateaus at high and low  $G$  (violet) and middle and low  $G$  (brown). Both combinations were observed in around 2-3% of all traces with plateaus.

### Conductance for OPE4-OMe

For compound **OPE4-OMe**, different behaviors were found when the percentage of traces displaying plateaus was changed significantly (by using different solution concentrations to deposit the molecules over the STM substrates from  $10^{-4}$  to  $10^{-7}$  M). Figures S6a and d and Figure S7a show that the overall molecular signal appears at higher conductance values when a high percentage of the traces presents plateaus (around 80%) than when the percentage is low (around 20%). A high rate of traces with plateaus is associated with a large density of molecules in the surface of the electrode apexes that, depending on the compound, might lead to junctions with several molecules stacked in parallel between the electrodes.<sup>4</sup> To investigate this possibility, we carried out the clustering-base analysis explained in the previous section in the **OPE4-OMe** recorded traces. In both regimes, we distinguished two groups. The first one, A (see Figure S6b and e), was formed by flat plateaus of equivalent conductance and plateaus length for both high and low rate of traces with plateaus (see also S7b). The reproducibility and flat-plateau profile of these traces allow us to attribute them to junctions with a single molecule fully extended between the electrodes, and it is therefore our signal of interest. On the other hand, the second group, B, was quite different depending on the rate of traces with plateaus. Only when this rate of plateaus is high, about half of the traces display sloping plateaus of higher conductance (Figure S6c), which suggest that these are indeed due to junctions with several molecules in parallel between the electrodes. Meanwhile, when the rate of plateaus is low, the second group is formed by traces with rather short plateaus forming after the electrodes have been separated more than 1.5 nm (Figure S6f). This profile suggest that a single molecule is closing the molecular junction between two already well separated electrodes.<sup>5</sup> The plateaus in this group appear at the same conductance value as those of group A (see Figure S6e and f), reinforcing the argument

---

<sup>4</sup> (a) D. Miguel, L. Álvarez de Cienfuegos, A. Martín-Lasanta, S. P. Morcillo, L. A. Zotti, E. Leary, M. Bürkle, Y. Asai, R. Jurado, D. J. Cárdenas, G. Rubio-Bollinger, N. Agraït, J. M. Cuerva and M. T. González, *J. Am. Chem. Soc.*, 2015, **137**, 13818. (b) M. T. González, X. Zhao, D. Z. Manrique, D. Miguel, E. Leary, M. Gulcur, A. S. Batsanov, G. Rubio-Bollinger, C. J. Lambert, M. R. Bryce and N. Agraït, *J. Phys. Chem. C*, 2014, **118**, 21655.

<sup>5</sup> L. Venkataraman, J. E. Klare, I. W. Tam, C. Nuckolls, M. S. Hybertsen and M. L. Steigerwald, *Nano Lett.*, 2006, **6**, 458.

that the conductance of group A corresponds to the single-molecule conductance of **OPE4-OMe**. Its 2D conductance profile, main conductance value and plateau-length distribution agrees very well with those of the low-*G* group of **OPE4-pym**. For the latter, we observed also traces with sloping plateaus as those of Figure S6c, but in a lower percentage, corroborating that side chains can promote packing in OPEs.<sup>4b</sup>

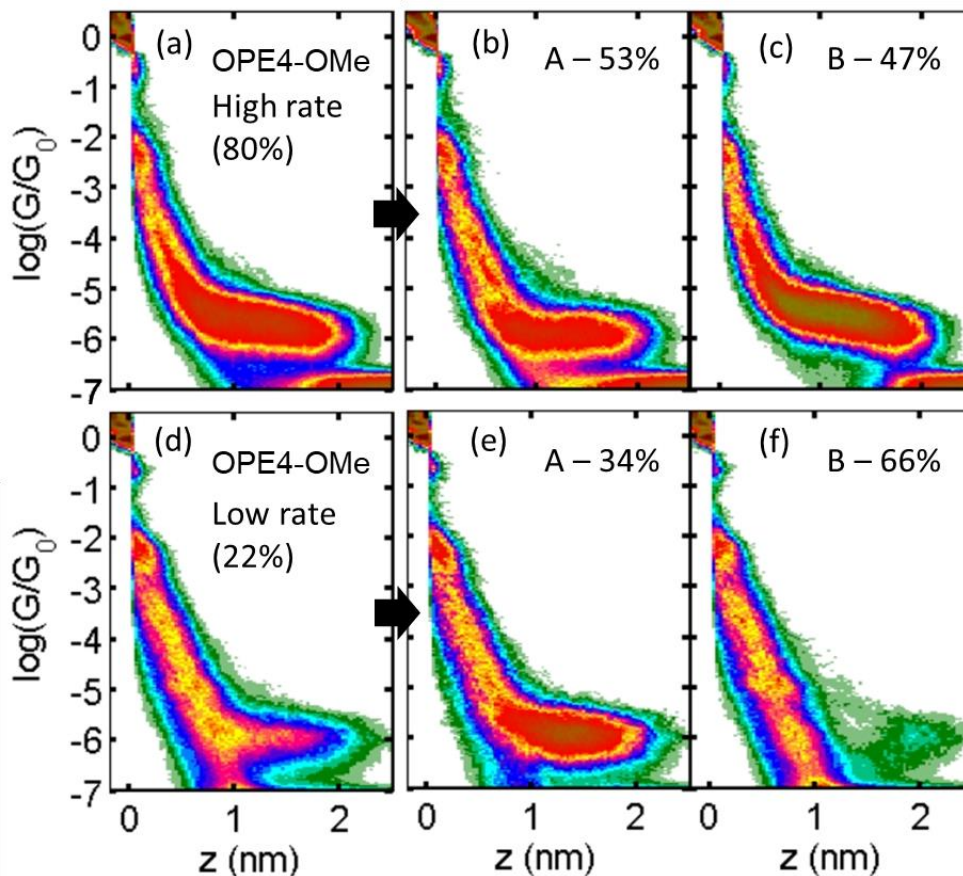


**Figure S6.** 2D histogram for **OPE4-OMe** at high (a) and low (d) rate of traces displaying plateaus. For these two different scenarios, two groups of breaking profiles were found. In both cases, group A (b and e) is formed by flat plateaus corresponding to a single molecule fully extended between the electrodes, while group B (c and f) corresponds to different processes in each case.

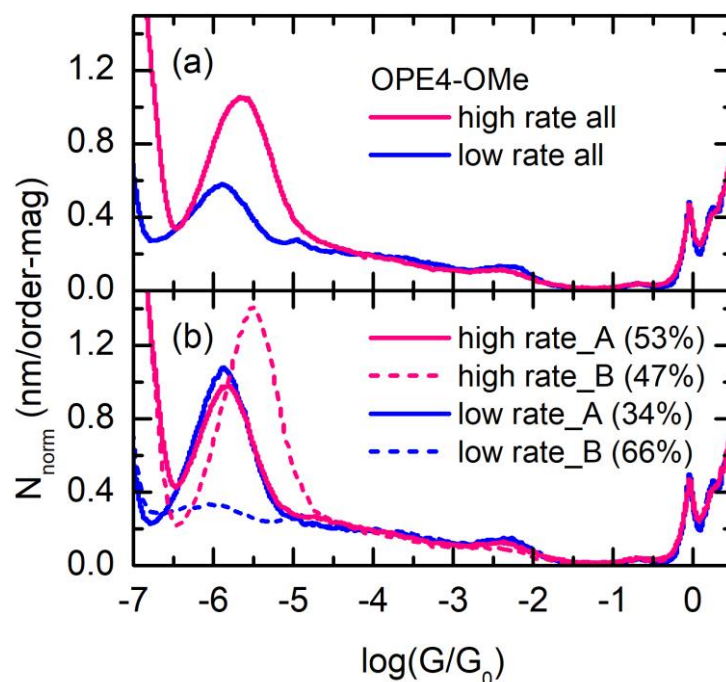


**Figure S7.** 1D histograms for **OPE4-OMe** at low (blue) and high (pink) and low (blue) rates of traces displaying plateaus, before (a) and after (b) separation of the total traces in groups according to their different conductance profiles.

#### Conductance for OPE3/S-pym

Figure S8 shows the 2D histogram obtained for **OPE3/S-pym**, corresponding to the 1D histogram shown in Figure 4c of the main text. This compound produced a clear signal with plateaus in 36% of the traces. Its mean value is at  $\log(G/G_0) = -5.0 \pm 0.45$ , approximately the expected value considering the equivalent compound of two rings previously measured in reference 4a (compound 7), with a mean conductance of  $\log(G/G_0) = -3.7 \pm 0.26$ , and a typical decay factor for OPEs of around 1 order of magnitude per phenyl ring ( $\beta = 3.2 \text{ nm}^{-1}$ ).<sup>6</sup>

<sup>6</sup> V. Kaliginedi, P. Moreno-García, H. Valkenier, W. Hong, V. M. García-Suárez, P. Buiters, J. L. H. Otten, J. C. Hummelen, C. J. Lambert and T. Wandlowski, *J. Am. Chem. Soc.*, 2012, **134**, 5262.

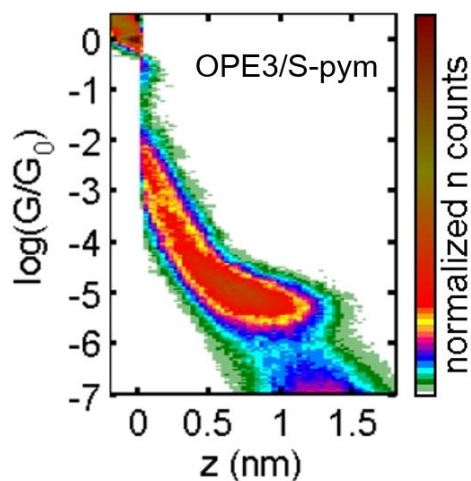


**Figure S8.** 2D histogram for **OPE3/S-pym**. The corresponding 1D histogram and plateau-length distributions are shown in Figure 4 of the main text.

#### Conductance for OPE2/S-pym

Single-molecule experiments performed for **OPE2/S-pym** gave rise to 9% of  $G$ - $z$  traces displaying plateaus. The 2D histogram of these traces is shown in Figure S9a, while the 1D histogram is shown in Figure 4e of the main text. The histograms show a molecular signal quite broad in conductance, which we also analyzed using the clustering analysis. This resulted in two different conductance clouds showed in Figure S9b and c. The first one, occurring with a higher probability (78% of the traces with plateaus), is formed by sloping plateaus between  $\log(G/G_0) = -2$  and  $-3$ , while the second less probable one contains flatter plateaus at a higher conductance. Although the origin of these sets of signals observed for **OPE2/S-pym** is not clear, the low percentage of total traces displaying plateaus (9%) discard the possibility of being due to several molecules in the junction. Otherwise, this effect seems similar to that observed for pyridine-linked compounds, which display two different sets of signals, particularly well-differentiated for short molecules as bipyridine.<sup>7</sup> We therefore hypothesized that the two groups can be originated by two different binding configurations of the bond gold – pyrimidine ring, maybe also with the contribution of the neighbor alkyne group. In

<sup>7</sup> (a) S. Y. Quek, M. Kamenetska, M. L. Steigerwald, H. J. Choi, S. G. Louie, M. S. Hybertsen, J. B. Neaton and L. Venkataraman, *Nat. Nanotechnol.* 2009, **4**, 230. (b) M. Baghernejad, D. Z. Manrique, C. Li, T. Pope, U. Zhurav, I. Pobelov, P. Moreno-García, V. Kaliginedi, C. Huang, W. Hong, C. Lambert and T. Wandlowski, *Chem. Commun.*, 2014, **50**, 15975. (c) M. Kamenetska, S. Y. Quek, A. C. Whalley, M. L. Steigerwald, H. J. Choi, S. G. Louie, C. Nuckolls, M. S. Hybertsen, J. B. Neaton and L. Venkataraman, *J. Am. Chem. Soc.*, 2010, **132**, 6817.

particular, the sloping plateaus of group A end at around  $\log(G/G_0) = -3.3$ , which is only slightly higher than the conductance value reported in the literature for the equivalent compound with a pyridine in ortho position instead of our pyrimidine in **OPE2/S-pym** ( $\log(G/G_0) = -3.6$ ),<sup>8</sup> suggesting an evolution on the coupling of the pyrimidine and the gold as the electrodes are separated.

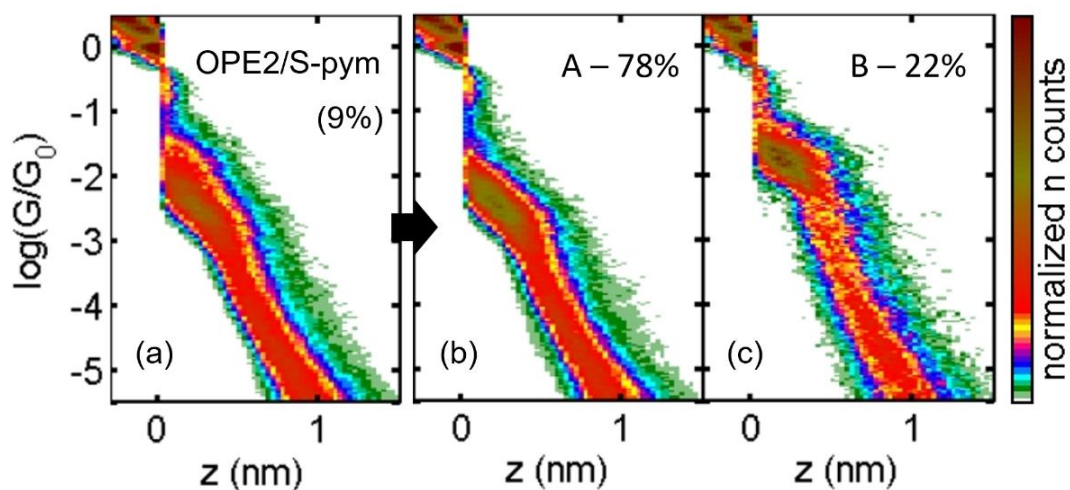


**Figure S9.** (a) 2D histograms for all traces with plateaus for **OPE2/S-pym**. (b) Independent 2D histograms for two separated groups of signals.

#### **4. ADDITIONAL THEORETICAL CALCULATIONS**

Figure S10 shows geometry 'f' in which **OPE3/S-pym** is connected to the lower gold electrode in a similar way as for the 3-ring fragment of **OPE4-pym** in geometry 'b' of the main text. These two structures are almost identical in the region between the two gold electrodes, but differ by way of the presence of the lower molecular branch in 'b', which is physisorbed on the lower electrode as well as being bonded to it through the lower S atom. Hence comparing these two structures provides us with information about the role of this lower molecular part on the electron transport. We observe that structure 'f' gives a lower conductance value ( $5.4 \times 10^{-4} G_0$ ) than that of 'b' ( $1.2 \times 10^{-3} G_0$ ). The lower conductance value of 'f' is partly due to the absence of the lower S–Au bond (which shifts the resonance to higher energies in 'b') and partly due to the lower

<sup>8</sup> X. Liu, S. Sangtarash, D. Reber, D. Zhang, H. Sadeghi, J. Shi, Z.-Y. Xiao, W. Hong, C. J. Lambert and S.-X. Liu, *Angew. Chem., Int. Ed.*, 2017, **56**, 173.

level of conjugation in the short molecule with respect to the long one (which in turn generates a larger HOMO-LUMO gap).

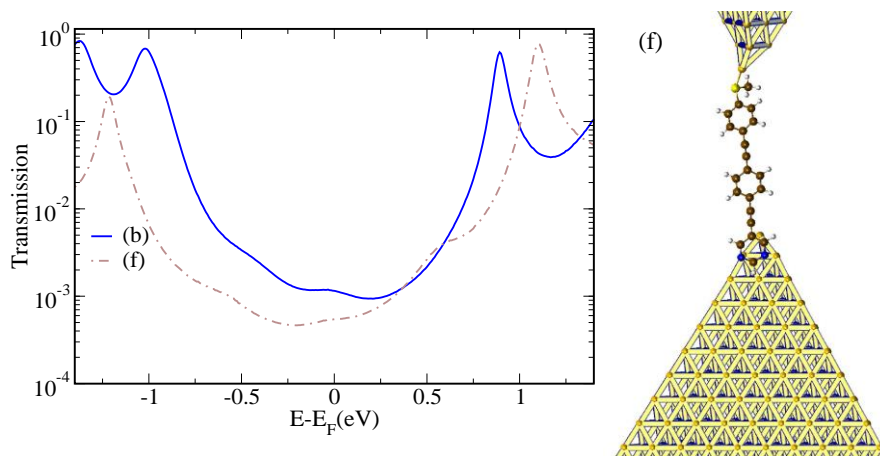


**Figure S10.** Transmission as a function of energy (left panel) for **OPE4-pym** in geometry ‘b’ of the main text and for **OPE3/S-pym** in the geometry ‘f’, shown in the right panel.

In Figure S11, we next show a comparison between the transmission curves of **OPE4-pym** in geometry ‘d’ of the main text and **OPE2/S-pym** in a position ‘g’ in which the heterocycle is physisorbed on the side of the gold electrode (as for the 2-ring fragment in ‘d’). Contrary to that observed in Figure S10, in this case the reference compound yields a higher conductance than **OPE4-pym** in geometry ‘d’. Indeed in our experiments, part of the traces of **OPE2/S-pym** (those in Figure S9c) present higher conductance than **OPE4-pym**.

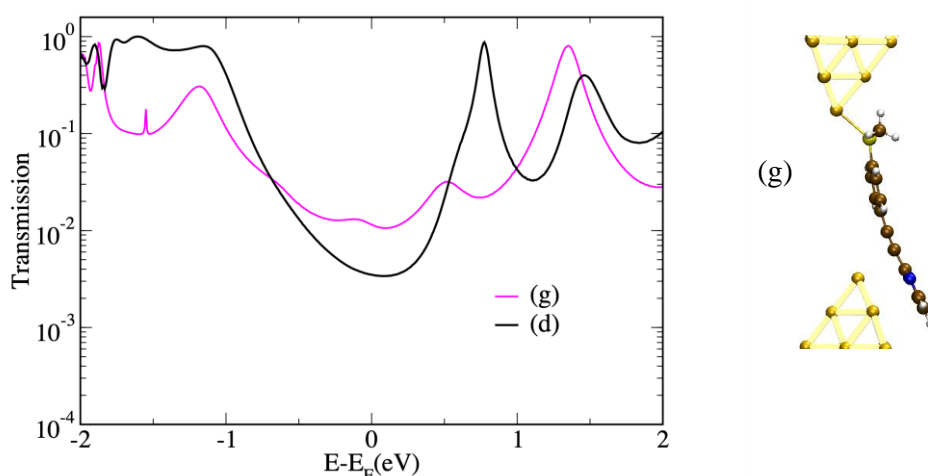


**Figure S11:** Transmission curves (left panel) for **OPE4-pym** in geometry ‘d’ of the main text and for **OPE2/S-pym** in a physisorbed geometry ‘g’ (right panel).

Finally, Figure S12 shows a geometry for **OPE4-pym** which was not considered in the main text. In this structure, the 3-ring fragment is attached to gold via an N–Au bond. The corresponding conductance value ( $2.6 \times 10^{-6} G_0$ ) is much lower than in the other cases. This is in agreement with what we observed for a short pyrimidine-based compound in the same configuration<sup>4</sup> and it is due to the *meta* binding configuration which is well known to lead to destructive quantum interference,<sup>9</sup> causing a strong antiresonance close to the Fermi level. By taking into account the well-known conductance overestimation arising from the DFT inaccuracies, we can conclude that the “real” conductance value of this geometry would be extremely small and probably hard to detect in the experimental measurements (as it would fall below the limit of the measurable range).

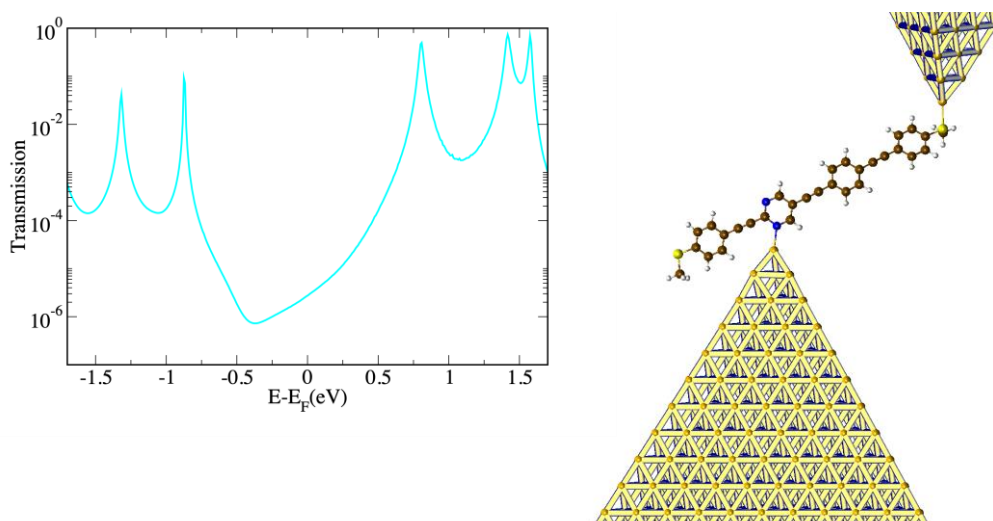


**Figure S12.** Transmission as a function of energy (left) for **OPE4-pym** in a configuration in which it is attached to one of the two electrodes only via a N–Au bond (right).

<sup>9</sup> M. H. Garner, G. C. Solomon and M. Strange, *J. Phys. Chem. C*, 2016, **120**, 9097.